| | |
|---|---|
| (51) International Patent Classification 5 : **A1** | (11) International Publication Number: **WO 94/01785** |
| **G01R 33/20** | (43) International Publication Date: 20 January 1994 (20.01.94) |

(21) International Application Number: PCT/US93/04574

(22) International Filing Date: 13 May 1993 (13.05.93)

(30) Priority data:
07/912,149     10 July 1992 (10.07.92)     US

(60) Parent Application or Grant
(63) Related by Continuation         07/912,149 (CIP)
US                                   10 July 1992 (10.07.92)
Filed on

(71) Applicant *(for all designated States except US)*: DOTY SCIENTIFIC, INC. [US/US]; 700 Clemson Road, Columbia, SC 29223-4300 (US).

(72) Inventor; and
(75) Inventor/Applicant *(for US only)* : DOTY, F., David [US/US]; 700 Clemson Road, Columbia, SC 29223-4300 (US).

(74) Agents: OPPEDAHL, Carl et al.; Oppedahl & Larson, 1992 Commerce Street, Suite 309, Yorktwon Heights, NY 10598-4412 (US).

(81) Designated States: AU, CA, JP, US, European patent (AT, BE, CH, DE, DK, ES, FR, GB, GR, IE, IT, LU, MC, NL, PT, SE).

(54) Title: SOLENOIDAL, OCTOPOLAR, TRANSVERSE GRADIENT COILS

(57) Abstract

A structure provides a gradient field useful in magnetic resonance imaging. Axially aligned, solenoidal-like coils (405) are symmetrically distributed around the perimeter of the bore of a superconducting magnet in an MRI system so as to produce transverse gradients in the X and Y directions with exceptionally high efficiency and exceptionally low acoustic noise. Opposed solenoidal endcoils (401) may be added to reduce axial flux leakage by generating an axial quadrupolar field. Radially aligned coils may be positioned near each end of the axial coils to reduce leakage flux by adding a transverse quadrupolar field to form a resulting octopolar field. Typically, the solenoid-like coils have a mean radius of about 15 % of the radius of that of the imaging ellipsoidal region. A thick-walled stainless steel, copper and resin cylinder (701-703) may be used to simplify gradient shielding problems. Silver plated bronze or stainless steel sheet is used as an rf shield (717, 718).

-1-

## Description

## Solenoidal, Octopolar, Transverse Gradient Coils

### Field of the Invention

The field of this invention is electromagnetic
coils for the purpose of efficiently generating
transverse gradients, especially in magnetic resonance
imaging (MRI) and other gradient techniques employing a
5      superconducting magnet.

### Background of the Invention

A large number of gradient-based MRI techniques
have been developed since its independent invention by
Paul Lauterbur and Peter Mansfield in 1973, following
10     the invention of the static technique of Damadian in
1972. Most modern MRI systems utilize a super-
conducting solenoid to establish a uniform $B_0$ (or $B_z$)
over the imaging volume. This results in the magnetic
field being colinear with the path available for sample
15     access. Coils are then required to produce monotonic
(preferably linear) gradients in $B_z$ with respect to x,
y, and z over the sample region during precisely
determined pulse sequences. The transverse gradients
($\delta B_z/\delta x$, $\delta B_z/\delta y$) in the prior art have generally been
20     established by symmetrically located sets of saddle
coils, similar to those first described by Golay in
U.S. Patent No. 3,569,823 or by related planar coils as
disclosed by Roemer, U.S. Patent No. 4,926,125 and
Morich et al., U.S. Patent No. 5,036,282. Maxwell
25     pairs are universally used to generate the axial
gradient, notwithstanding the incorrect usage of the
word "toroidal" by Frese and Siebold in U.S. Patent No.
4,468,622. The instant invention achieves order-of-
magnitude improvements in several critical parameters
30     for transverse gradient coils: acoustic noise, DC

gradient efficiency, and high-speed switching
efficiency.

The closest prior art to the instant invention, in
terms of magnetic field configuration, appears to be
5    the trapezium loops for use with an electromagnet, as
disclosed in the article "Magnetic Field Gradient Coils
for NMR Imaging" by Bangert and Mansfield in *Journal
Physics, E, 15*, 235 (1982). The semi-cylindrical
concept depicted by Mansfield in U.S. Patent No.
10   4,165,479, while having some similar features, is not
closely related, as its major field component is
orthogonal to $B_z$.

The gradient pulses induce eddy currents and
vibrations in nearby conducting structures (especially
15   in flimsy shields, in the cryostat, and in light-weight
rf coils) which perturb the field homogeneity following
the pulses with time and spatial dependencies that are
not easily characterized. Active shielding coils, were
first publicly disclosed by Mansfield in 2/1986 at
20   approximately the same time that Roemer filed the
patent application which resulted in U.S. Patent No.
4,737,716. Prior independent work was underway at Doty
Scientific, who shipped the first such commercially
available coils in 1/1987. Figure 1 approximately
25   depicts typical shielded Golay coils to generate $\delta B_z/\delta x$
in the sample in the vicinity of the origin. A similar
set of concentric coils, rotated 90°, is used to gen-
erate $\delta B_z/\delta y$. Figure 2 shows second-order shielding of
the Maxwell pair, or anti-Helmholtz coils, as used to
30   generate linear $\delta B_z/\delta z$ near the origin. Gradient coils
**201, 202** at mean location $z\approx\pm r_f$ have about 2.5 times the
amp-turns of shield coils **203, 204** when $s\approx0.3r_f$. Axial
shield coils **205, 206** have about one-tenth the amp-
turns of the gradient coils. Gradient linearity of
35   ±20% is achieved over a sphere of radius $0.7r_f$, and
leakage flux through a cylinder of radius $1.4r_f$ is

reduced by a order of magnitude compared to the
unshielded case. Higher-order shielding achieves
another order-of-magnitude reduction in leakage, but
shielding techniques have never fully measured up to
5   original expectations because of motion-related
artifacts, especially ghosting in the phase-encoding
direction and battle-zone levels of acoustic noise.

Recovery time is often found to increase quadra-
tically with pulse amplitude, indicating it is related
10  more to motion than to eddy currents. It is in fact
arguable that eddy currents per se are no longer a
significant problem with typical shielded coils and
optimized multi-exponential high-pass compensation that
includes first-order cross terms as described by Van
15  Vaals and Bergman, but rather the vibrations produced
by the eddy currents in passive shields are the cause
of residual image artifacts, as the time constants of
the high-order eddy currents in passive shields are
generally much less than the mechanical vibration time
20  constants. Kondo et al. in U.S. Patent No. 5,055,789
disclose a partial solution to the image artifact
problem.

The gradient coil design problem is fundamentally
limited by the conflicting requirements of fast res-
25  ponse and reasonable field linearity (spatially con-
stant gradients) over the sample volume. The major
technical problems center around the following:
(1) limited available space because of economic
considerations, (2) motion-induced artifacts arising
30  from the finite stiffness and mass of the coil support
structure, (3) practicable coil winding (or etching)
techniques, (4) acoustic noise abatement, and (5) heat
dissipation.

The conflicting technical requirements may be
35  partially addressed by means of local planar gradient
coils with highly non-linear response, as disclosed by

-4-

Roemer, U.S. Patent No. 4,926,125.  By adding distor-
tion correction algorithms to the image processing, it
is possible to utilize gradients with ±40% to ±60%
non-linearity on one axis in applications where high
spatial resolution is required only over a small
portion of the image.

The following parameters generally need to be
specified for gradient coil systems: gradient coeffi-
cient $\alpha$ (T/Am) (sometimes called gradient efficiency in
the prior art), imaging ellipsoid radius $r_i$ (m) and
axial length $h_i$ for a specified linearity, inductance $L$
(H), resistance $R_E$ ($\Omega$), maximum continuous power dissi-
pation P (W), maximum pulse current $I_P$ (A) in a speci-
fied $B_0$, recovery time $T_D$ (s) for a specified pulse, and
acoustic noise for a specified pulse sequence in a
specified field.

For the fastest imaging techniques, Echo Planar
Imaging (EPI) and related techniques, the most impor-
tant parameters are acoustic noise, recovery time, and
gradient power.  EPI can produce complete 2-dimensional
images in 30 ms and repeat the process several times
per second, compared to minimum imaging times of sev-
eral minutes for conventional spin-echo techniques.  In
addition to the enormous prospects for increased
patient throughput in MRI, EPI allows realtime moni-
toring of heart valve function and even realtime
analysis of brain response to visual and auditory
stimuli.

Although EPI was first described 15 years ago, it
has seldom been used because prior art gradient coils
(a) may require megawatts of gradient driver power on
the frequency-encoding axis, (b) generate sound pres-
sure levels that are painful and damaging to the
patient's hearing, (c) produce motion-related artifacts
that cannot be fully removed even with the most
sophisticated image post-processing, and (d) require

high power audio amplifiers costing up to several
million dollars. A recent experimental demonstration at
0.5 T required nearly half a megawatt (at 10% duty
cycle) at one kHz, and others have proposed the use of
2 MW at 5 kHz, 1.5 T, and 50% duty cycle for slice-
interleaved techniques. The above problems may be
partially addressed using a tuned transverse gradient
with sinusoidal (monochromatic) current; but the
conventional gradient coil has very low electrical Q;
and there are penalties in SNR (signal to noise ratio)
and heat dissipation. Also, computational analysis
becomes more complex, but that objection is trivial.

While the Maxwell z-gradient is considerably more
efficient than the Golay transverse gradient, the
frequency-encoding gradient must be in the plane of the
image, which often must be transverse for medical
reasons. Hence, order-of-magnitude improvements are
needed in transverse gradients.

The image artifact problem can begin to be appre-
ciated by noting that while the frequency-encoding
gradient may be driven with a 500 kW trapezoidal wave
form, the phase-encoding gradient is being driven with
short "blips" of several kilowatts at very low duty
cycle, and the slice-selection axis is nulled. It is
quite easy for non-linear, vibration-dependent cou-
plings between the frequency-encoding axis and the
other axes to destroy the required degree of ortho-
gonality between the axes and produce phase-related
artifacts. Moreover, cylindrical asymmetries in rf and
gradient shields can make the orthogonality frequency
and amplitude dependent.

The availability of better image processing and
distortion correction techniques suggests that the
linearity standard be increased to ±20%, compared to
the more typical ±10% value for prior art whole-body
systems. (Linearity in prior art MR microscopy is

typically ±4% or better because the rf coils require a
relatively large exterior dead space, which necessarily
makes gradient linearity very good over the small
sample region.)  Increasing the non-linearity allowance

5    from ±10% to ±20% increases the imaging volume by
typically 50%.  It is still important that the field be
monotonic, but the method of Schenck et al. in U.S.
Patent No. 4,646,024 results in relatively poor switch-
ing efficiency, intolerable acoustic noise, and unman-

10   ageable motion-related artifacts.

         Designing for large gradient non-linearity with
very fast switching capability places increased (though
inconsequential) computational demands on the image
processing and may result in some increased variation

15   in SNR over the final image.  However, the enormous
bandwidth (several MHz) of high-resolution EPI (and
other more advanced techniques) can reduce the imaging
time by two or three orders of magnitude without plac-
ing unrealistic demands on modern computers since

20   computational power per cost has increased at the rate
of 40% per year for the past seven years and that rate
is expected to continue for several more years.

         Magnetic energy storage estimates can be enlight-
ening.  Assume gradients of 1 T/m over an imaging

25   sphere of 14-mm radius (±20% linearity) for a typical
solids microscopy application using a transverse
gradient coil of 45-mm diameter.  We might then expect
maximum gradient fields of about 0.02 T (50% more than
the sample's maximum) over a volume of perhaps 60 ml

30   (6 times the sample volume); hence, 0.01 J.  Switching
this field in 100 $\mu$s would require 100 W, assuming
relatively low resistive loss, which can easily be
achieved.  In practice, using conventional shielded
gradient coils, the inductive energy ($I^2L/2$) is larger

35   than suggested by simple energy estimates as above by a
factor of twenty to one hundred.

While most of the wasted magnetic energy in Golay
coils is external to the patient in MRI, the unusable
magnetic energy (the integral of the rms value of $B_x+B_y$)
over the patient may be an order of magnitude larger

5    than the usable field (the integral of the rms value of
$\delta B_z/\delta x$ or $\delta B_z/\delta y$ over the image volume). It is the
switching of this enormous non-gradient field from the
Golay geometry that causes the sensory stimuli in
patients during EPI experiments and limits clinical

10   applications. It is also this non-gradient field that
is responsible for virtually all of the eddy currents
and vibrations induced in the rf coils, as the desired
gradient field is axial and its dipole moment is zero.
           Conventional transverse gradient coils have always

15   been designed from the deeply ingrained perspective
that a single large coil is more efficient and less
costly than a collection of smaller coils. This notion
may be true most of the time, but not when it comes to
complex field geometries. Maxwell's laws make it

20   impossible to design coil systems that generate single
field gradients (they must come at least in pairs) but
it is not necessary to have large orthogonal field
components.
           Some prior gradient coil designs have also suf-

25   fered under the false notion that there is an inherent
advantage with very low inductance coils. Higher
inductance (more turns) requires higher voltage, but
not higher power (VA) for the same switching time. In
fact, reducing inductance below 100 $\mu$H is detrimental

30   as lead inductance and transmission line problems then
become significant. Coil orthogonality (for isolation)
and net force cancellation both dictate that integral
numbers of turns be used in all coil sets and coil
subsets. Hence, the accuracy of the shielding is

35   limited from this quantization. The more turns, the
more precisely the gradients can be shielded. Optimum

number of turns is thus determined largely by the VA
characteristics and economics of available power
devices, magnetic shielding accuracy requirements, and
standard wire insulation practice, making 250 V to 800

5    V (peak differential voltage for a balanced line) at 10
A to 100 A best for large systems.  Optimum inductance
is typically 0.2 to 1 mH.


## Summary of the Invention

10        Axially aligned, solenoidal-like coils are sym-
metrically distributed around the perimeter of the bore
of a superconducting magnet in an MRI system so as to
produce transverse gradients in the x and y directions
with exceptionally high efficiency and exceptionally

15   low acoustic noise.  Opposed solenoidal end-coils may
be added to reduce axial flux leakage by generating an
axial quadrupolar field.  Radially aligned coils may be
positioned near each end of the axial coils to reduce
leakage flux by adding a transverse quadrupolar field

20   to form a resulting octopolar field.  Alternatively,
Golay-type coils may be used for the transverse quadru-
polar field with some improvement in efficiency.
Typically, the solenoidal-like coils have a mean radius
of about 15% of the radius of that of the imaging

25   ellipsoidal region.  The cylindrical rf shield between
the imaging ellipsoid and the gradient coils may have
smaller radius at the ends than near the center.
Radial forces in axial gradient systems are largely
canceled by concentric support members between the

30   gradient and shield coils.  A thick-walled stainless
steel, copper, and resin cylinder may be used to
simplify gradient shielding problems.  Silver plated
bronze or stainless steel sheet is used as an rf
shield.

35

## Brief Description of the Drawings

The invention will be described with respect to a drawing, of which Figure 1 illustrates the prior-art, shielded, Golay-type, transverse gradient coils.

Figure 2 is a longitudinal cross section of the prior-art, shielded, Maxwell-pair axial gradient coils.

Figure 3 discloses a pair of opposed solenoidal octopolar coils in longitudinal cross section with typical lines of flux producing a transverse gradient.

Figure 4 depicts a quadrant of solenoidal coils with octopolar field inside a passive gradient shield.

Figure 5 discloses an octopolar transverse gradient coil assembly for a single transverse axis.

Figure 6 discloses a shielded axial gradient coil system with concentric support members.

Figure 7 is a longitudinal cross section of a complete x-y-z gradient coil system with central inside radius larger than end inside radius.

Figure 8 is a schematic MRI system representation.

Figure 9 discloses a c-coil transverse gradient system.

Figure 10 discloses a U-coil transverse gradient system.

Fig. 11 shows an axial end view of the structure of Fig. 5;

Fig. 12 shows an alternative embodiment for a coil assembly; and

Fig. 13 shows an alternate embodiment for a coil assembly having inclined solenoidal windings.

Throughout the figures, like elements have been shown where possible with like reference numerals.

## Detailed Description of the Preferred Embodiment

Qualitative comparisons of various gradient coil geometries of different sizes are often misleading because of the complex expressions for power,

inductance, resistance, and gradient coefficient and
the varying degrees of sensitivity to coil motion. For
example, power is often proportional to radius to the
fifth power for constant winding thickness and voxel
5    size. But power may be linear with radius for constant
number of voxels and constant relative winding thick-
ness, depending on the relative significance of $\gamma G r_i T_2$
and SNR in determining spatial resolution, where $\gamma$ is
the magnetogyric ratio, $G$ is the magnetic field grad-
10   ient (T/m), and $T_2$ is the spin-spin relaxation time (s).
Thus, it is useful to develop dimensionless figures of
merit for comparison of various gradient coil systems
of various sizes.

     We begin a dimensionless analysis by defining a
15   switching figure-of-merit, or switching efficiency,

$$\eta_s = \frac{U_S}{U_T} \, , \qquad\qquad (1)$$

where $U_S$ is the gradient energy over the maximum sample
volume of $\pm 20\%$ field linearity and $U_T$ is the total
gradient energy over all space.
20

$$U_s \approx g \, (\alpha I r_i)^2 \frac{V}{2 \mu_0} , \qquad\qquad (2)$$

where $g$ is a dimensionless integration factor as
implicitly defined in the above equation and is
approximately equal to 0.2 for typical ellipsoidal
25   sample geometry ($g=0.33$ for a cube), $V$ is the maximum
imaging volume (m$^3$), $\mu_0$ is the permeability of free
space, and $\alpha$ is the mean gradient coefficient (T/Am).

$$U_T = I^2 \frac{L}{2} \, , \qquad (3)$$

hence, for convenience, we re-define the switching efficiency as

$$\eta_S = \frac{\alpha^2 r_i^4 h_i}{2\mu_0 L} \, , \qquad (4)$$

5     where $h_i$ is the axial imaging length.  The above
efficiency has typical numeric value between 0.001 and
0.008 for shielded Golay coils, or 0.005 to 0.03 for
Maxwell pairs and quadrupolar coils for use in magnets
with transverse $B_0$.  This suggests at least an order-
10    of-magnitude improvement in switching efficiency should
be possible for transverse gradients with novel coil
geometries.
        Next we define a low frequency (LF) efficiency $\eta_L$
by comparing the quality of the gradient coil system to
15    that of a simple solenoid.

$$\eta_L = \frac{P_0}{P_G} \, , \qquad (5)$$

where $P_0$ is the power required to generate a peak
magnetic field of $B_G$ in a copper solenoid of radius $r_i$
and length $2r_i$ at angular frequency $\omega_1$ at room tempera-
20    ture, and $P_G$ is the power required to generate a peak
gradient of $B_G$ at radius $r_i$ using the gradient coils for
the same conditions.
        It is easily shown from basic principles and
definitions (and is experimentally confirmed) that

-12-

$$P_0 \approx \frac{B_G^2 \omega_1 V}{\mu_0 Q_0} , \qquad (6)$$

where $Q_0$ is the ratio of the reactance to the series
resistance at frequency $\omega_1$. The LF Q at room
temperature of a copper solenoid (with full surface
5   coverage) with length equal to its diameter is easily
estimated as

$$Q \approx 5 r_i \sqrt{\omega_1} \qquad \left[\frac{s^{0.5}}{m}\right], \qquad (7)$$

where we assume the copper thickness to be greater than
twice the skin depth $\delta$ at the test frequency. (This
10  condition is not met in small coils at low frequencies,
as $\delta = 6.5$ mm at 100 Hz.) Hence,

$$P_0 \approx B_G^2 \sqrt{\omega_1} \frac{r_i^2}{\mu_0} \qquad \left[\frac{m}{s^{0.5}}\right], \qquad (8)$$

$$P_G = I^2 R_E = B_G^2 \frac{R_E}{\alpha r_i^2} \qquad \left[\frac{m}{s^{0.5}}\right], \qquad (9)$$

where the constants in the above equations have units
15  as indicated in brackets so as to maintain SI
consistency and arise from the skin depth of copper at
room temperature as a function of frequency. We now
re-define $\eta_L$ as the ratio of the above expressions for
$P_0$ and $P_G$:

$$\eta_L = \frac{\sqrt{\omega_1}\, \alpha^2 r_i^4}{\mu_0\, R_E} \qquad \left[\frac{m}{s^{0.5}}\right]. \qquad (10)$$

At 100 Hz, this evaluated to 0.0004 for a typical
prior-art transverse coil designed for $r_i$=42 mm (the
copper thickness was about half of the skin depth) but

5   values below 0.0001 are typical for large planar
transverse gradient coils. Typical values for
Maxwell-pairs are near 0.002, and there is usually
little justification for higher LF efficiency. It
would appear that there is room for at least an

10  order-of-magnitude improvement in LF efficiency of
transverse gradient coils. A more accurate figure of
merit governing efficiency during EPI is the product of
$\eta_S$ and the electrical Q at the switching frequency
(e.g., 1600 Hz), but that cannot be determined without

15  knowledge of the winding thicknesses and surface areas,
which are rarely given in the published literature.

    Coil motion is generally the most troublesome
design limitation - perhaps because it is more diffi-
cult to construct a generalized figure of merit that

20  satisfactorily accounts for vibration of the gradient
coils and of the nearby structure. The governing
equations change radically depending on whether most of
the energy in the gradient pulse spectrum is below or
above the fundamental mechanical mode to which it is

25  strongly coupled.

    The saddle coils in conventional Golay-type
transverse gradient coils in a uniform external
magnetic field develop opposite torques which cause
the cylindrical coilform to bow in the plane of the

30  z-axis and the desired gradient.

    For very small coil systems, the LF limit is
usually applicable -- $\omega_g \ll \omega_b$, where $\omega_g$ corresponds to the
dominant component in the gradient power spectrum and $\omega_b$

is the fundamental (symmetric bowing) vibration mode.
For a cylindrical coilform supporting conventional
transverse gradient coils, the form experiences
balanced bowing torques equivalent to a transverse
5       force $F_B$ at the center (and $-F_B/2$ at each end) approxi-
mately equal to $n_t I B_0 r_f$, where $n_t$ is the total number of
turns (4 quadrants) and $r_f$ is the mean radius of the
coilform.  The bowing stiffness $k_b$ (N/m) for elastic
(Youngs) modulus $Y$, wall thickness $w$ (where $w \ll r_f$), and
10      axial coilform length $h$ is given approximately by

$$k_b \approx 100 \frac{Y r_f^3 w}{h^3} \; . \tag{11}$$

The bowing mode $\omega_b$ of a medium-walled cylindrical
coilform, heavily loaded at both ends (the typical
case), is approximately as follows:
15

$$\omega_b \approx 5 \frac{r_f c}{h^2} \; , \tag{12}$$

$$c = \sqrt{\frac{Y}{\rho}} \; , \tag{13}$$

where $\rho$ is the mean wall density and $c$ is the acoustic
velocity.  (For very thin walls, surface modes occur at
20      lower frequencies.  For very thick walls, the
coefficient in equation [12] drops to about 3.)
For an axially aligned solenoidal coil in a
uniform external field, the Lorentz forces are radial.
The radial stiffness of a thin-walled cylinder is

-15-

$$k_r = \frac{2\pi h Y w}{r_f}. \qquad (14)$$

Thus, the fundamental radial mode $\omega_r$ of a thin-walled cylinder is

$$\omega_r \approx \frac{c}{r_f}. \qquad (15)$$

5      The mechanical energy $U_M$ in the LF regime is approximately $F^2/2k$. It is independent of the pulse length, and seldom significant, as $k$ can be made quite large.

        For the typical case of high-power copper coils
10  epoxied into grooves cut into fiberglass forms, it is difficult to estimate effective $k$ and $m$ (or $Y$ and $\rho$) from detailed moment analysis. The fundamental transverse mode may be less than one-third that calculated for a fiberglass cylinder as the transverse
15  stiffness can be substantially degraded.

        The radial mode is less affected by the addition of a tightly wound copper winding on a cylindrical form than is the transverse mode. Thus, for the typical case where $h=4r_f$, with coil mass several times that of
20  the form mass, the transverse frequency may be one tenth of the radial frequency. Table I gives some properties of typical materials.

| TABLE I Materials Properties | | | |
|---|---|---|---|
| Materials | Density Mg/m$^3$ | Modulus GPa | c m/s |
| (a) PEEK | 1.3 | 3.6 | 1700 |
| (b) G-10 | 1.5 | 10 | 2600 |
| (c) N66-60G | 1.7 | 20 | 3400 |
| (d) Copper | 9.0 | 130 | 3700 |
| (e) Macor | 2.5 | 62 | 5000 |
| (f) SS304 | 8.0 | 190 | 5000 |
| (g) E-GF | 2.6 | 72 | - |
| (h) Zirconia | 5.7 | 220 | 6200 |
| (i) WC | 15.6 | 660 | 6500 |
| (j) Nextel 440 | 3.1 | 220 | - |
| (k) Alumina | 3.9 | 380 | 9900 |
| (l) PAN-50 CF | 1.8 | 380 | - |

NOTES:    (a) Polyetheretherketone; (b) Glass cloth
reinforced epoxy; (c) Nylon-6/6, 60% glass fiber; (e)
machinable glass, Al-B-Si-K-F-O, Corning Glass Works;
(f) stainless steel alloy; (g) standard E-glass fiber;
(h) partially stabilized with MgO; (i) typical 1-micron
tungsten carbide powder; (j) Al-Si-B-O ceramic fiber,
3M; (k) 99.5%; (l) Thornel PAN carbon fiber.

For mid-sized to large systems ($r_f$ greater than 30
to 300 mm), $\omega_g$ is more likely to be comparable to $\omega_b$ or
a higher vibration mode, and it is here that problems
arise because the mechanical recovery time becomes long
compared to the gradient pulse length.  A conventional
transverse mid-sized gradient coil on a G-10 fiberglass
cylindrical coilform with $r_f$=35 mm, $h$=200 mm, and $w$=5 mm
would have $\omega_b/2\pi$ in the range of 600 to 1500 Hz,
depending on the amount of copper used - unless a
Maxwell pair for the z-gradient has been laid in

circumferential grooves on the same form, in which case
this mode could be below 300 Hz.

   For $\omega_g \gg \omega_b$, the motion during a single square pulse
of length $t_g$ (where $t_g < 1/\omega_b$) can be approximated as a

5  mass under the influence of a constant force since the
coilform stiffness is negligible compared to the coil's
inertia. The coil acceleration $a$ during the pulse is
$b_1 n_1 I r_f B_0 / m_c$, where $m_c$ is the coil mass per quadrant, $n_1$ is
the number of turns per quadrant, and $b_1$ is a dimension-

10 less function of the coil and coilform geometry with
typical value near 2. At the termination of the pulse,
the coil will be rotating with tip velocity $v = \pm a t_g$. Its
mechanical energy is kinetic $(mv^2/2)$. Hence, the mec-
hanical energy per quadrant $U_M$ from a single short

15 pulse is given by

$$U_M = \frac{(b_1 n_1 I r_f B_0 t_g)^2}{2m_c}, \tag{16}$$

since the effective moving mass (half of the coil mass
plus adjacent coilform) is comparable to $m_c$ for typical
Golay coils on fiberglass coilforms.

20     We define a dimensionless electro-mechanical,
high-frequency efficiency factor $\eta_{mh}$, which we desire to
be small:

$$\eta_{mh} = \frac{U_M}{U_S} = \frac{U_M}{\eta_S U_T}. \tag{17}$$

   For the typical case of negligible mutual

25 inductance between quadrants, the above ratio is the
same for a single quadrant as for the system, whether
series connected or parallel connected.

For shielded Golay coils, with the shield coils at
radius $r_f+s$, where $s$ is much less than $r_f$, the inductance
per quadrant is approximately

$$L \approx 8\mu_0 n^2 s . \qquad (18)$$

5    Thus,

$$\eta_{mh} \approx \frac{(r_f B_0 t_g)^2}{2\eta_s \mu_0 s m_c} . \qquad (19)$$

Clearly, relative mechanical energy during short
pulses is minimized by increasing $\eta_s$, $s$, and $m_c$ for a
given $B_0$ and $t_g$. Since $m_c$ would be expected to increase
10   as the third power of $r_f$, it might appear that
motion-related problems are reduced by increasing $r_f$.
However, $t_g$ (if inversely proportional to $B_G$) will
generally increase as the second, third, or even fourth
power of $r_f$ in large coils, depending on the severity of
15   acoustic noise and the amount of power that can be
justified. Thus, electro-mechanical energy in the
short-pulse limit typically increases very rapidly with
$r_f$ because the pulse lengths must increase.
          While *relative* high-frequency mechanical energy
20   per pulse ($\eta_{mh}$) is minimized by reducing the pulse
length, a proportional increase in the strength of the
gradient is required; hence, equation [16] shows that
$U_M$ remains unchanged. Moreover, the acoustic spectrum
would move into the more troublesome range where the
25   response would be similar to that of a conventional
loudspeaker. Another severe problem that often arises
for the high-frequency condition is that $\omega_g$ may be close
to $\omega_b$ or to one of the higher mechanical modes. The
single pulse analysis is invalid near resonance as the
30   initial velocity is no longer zero.

For the earlier mid-sized typical example with $B_0=2$ T, $t_g=0.5$ ms, $s=10$ mm, and $m_c=0.5$ kg, $\eta_{mh}$ evaluates to approximately 1.6, which means more energy is going into mechanical motion than into gradient energy in

5 the sample. In this case, however, the short-pulse approximations do not apply, as we are close to resonance. Thus, the actual situation is worse by a factor comparable to the mechanical Q, which has been found to lie between 3 and 20 for typical materials and

10 geometries.

The key to reducing both $U_M$ and relative mechanical energy is to change from the Golay geometry to the predominately solenoidal geometry of octopolar coils as shown in Figure 3. Each octopolar coil consists of a

15 central solenoidal coil **301**, two opposed solenoidal end coils **302, 303** adding a quadrupolar field in the z direction but not completely negating the dipolar field of the central solenoid **301**, and two cross coils **304, 305** adding a transverse quadrupolar field. The

20 magnetic flux for a properly wound pair of octopolar coils is mostly confined to the region between the coils as shown, which clearly produces the desired, monotonic field over a large sample region **306** inside sample coil **307**. The magnetic energy external to the

25 sample region is much less than in unshielded prior art, and the passive gradient shield **308** easily makes residual interactions with the main $B_0$ magnet **309** negligible. Compared to the prior art, the reduced transverse field components of the octopolar geometry

30 substantially reduces electrical hazard to the patient and asymmetrical eddy current interactions with the rf coil **307**. Before considering field linearity or the gradient magnitude, we look at the most significant prior-art limitations - mechanical energy and acoustic

35 noise.

        The most efficiently driven mode in the octopolar
solenoid is the radial mode, but the mean solenoid
radius $r_c$ is smaller by a factor of 4 to 15 than the
Golay $r_f$ for similar imaging radius $r_i$. Hence the
5    resonant frequency is 10 to 100 times higher than the
dominant mode for Golay-type coils. Gradient frequen-
cies may be increased by the same factor before getting
into the troublesome regime of equations [16] and [19].
The constant $b_1$ in equation [16] is increased to
10   approximately $\pi$ for a solenoid, and the coefficient in
equation [18] is significantly reduced, but this is
balanced by a similar increase in $\eta_s$. However, it is
now usually possible to stay below resonance, where
motion problems are easily eliminated by increasing the
15   stiffness.

        The small diameter of the solenoid makes it pos-
sible to select coilform materials that would be pro-
hibitively expensive to manufacture at the dimensions
required for a Golay coil, where fiberglass forms and
20   ceramic cement encapsulation are used. The radial mode
of the solenoid is maximized by choosing a material for
its coilform with high $Y$, such as alumina, mullite,
borosilicate glass, a machinable glass such as Macor,
or plastics highly loaded with high-modulus fibers of
25   ceramic, carbon, or glass.

        The radial force in a solenoid is simply $2\pi r_c n I B_0$
and the inductance of a long solenoid is $\mu_0 n^2 \pi r_c^2 / h$.
Hence, from equation [14] and the above, the mechanical
energy, $F^2/2k$, $U_M$ is

30

$$U_M = \frac{r_c L I^2 B_0^2}{\mu_0 Y w} . \tag{20}$$


        We may define a low-frequency electro-mechanical
efficiency factor $\eta_{ml}$ in the same manner as equation
[17] and show that it is

$$\eta_{ml} = \frac{2\,r_c B_0^2}{\eta_r \mu_0 Y W}. \qquad\qquad (21)$$

for the LF solenoid, which has typical value between
0.0001 and 0.01 for coils suitable for whole-body MRI
on high-modulus forms at high fields.

5      The cross coils 304, 305 will also weakly excite a
transverse vibration mode, which will be resonant at a
much lower frequency.  Since the pulse length would
often be short compared to the period of this trans-
verse mode, it may be beneficial to select a coilform
10     material that has high density, such as zirconia or a
composite loaded with a dense compound such as tungsten
carbide (WC) or zirconia fibers.  Fortunately, this
transverse mode is driven much less efficiently (by
about two orders of magnitude) than is the Golay $\omega_b$ for
15     the following reasons: (a) typically only 20% of the
total turns are transverse; (b) the mean axial dimen-
sion of the cross coils is about half that of Golay
coils, which reduces the torque correspondingly;
(c) the switching efficiency $\eta_s$ is increased by about a
20     factor of four; (d) the solenoidal coilform can easily
be made quite stiff and massive.

       Equation [21] is also approximately correct for
mechanical evaluation of Maxwell pairs used for the
z-gradient.  However, compared to the octopolar coils,
25     the z-gradient coil radius will be larger by a factor
of four to fifteen, the relative wall thickness may be
one tenth as large, $\eta_s$ may be larger by a factor of two,
and Y may be smaller by a factor of 2 to 40 for
manufacturing reasons.  Thus, the z-gradient may have
30     two orders of magnitude larger acoustic problems than
the transverse gradients - a reversal from the prior
art.  Fortunately, the z-gradient is normally used only

where the frequency components are very low, as in
slice selection or Gradient Enhanced Spectroscopy
(GES). An exception has been Pulsed Field Gradient
(PFG) diffusion measurement, which may now be performed
5    using a transverse octopolar gradient rather than the
z-gradient for minimum motion-related artifacts.

Referencing Figures 3 and 4, we begin the magnetic
analysis by considering a single, azimuthal quadrant of
identical octopolar coils, as depicted in Figure 4,
10   disposed adjacently in a sector with central inside
radius $r_f=1.3r_i$, outside radius $r_f+s=1.6r_i$, with a passive
cylindrical shield 308 at radius $r_f+s+\epsilon$ where $\epsilon$ is small
compared to $s$. The relative dimensions selected are
convenient for six or eight parallel octopolar coils
15   per quadrant, depending on the shape of the cross
section of the central solenoid 301. Instead of wind-
ing individual cross coils 304, 305 on each solenoidal
coilform, transverse saddle coils 401, 402 may be
threaded through the transverse holes 403, 404 in the
20   solenoidal coilform 405 to generate the transverse
quadrupolar field with some improvement in LF effi-
ciency but with no significant effect on other para-
meters. Transverse flux leakage may be reduced by
extending the central solenoid 301 into the transverse
25   coil region 406, 407. Transverse and axial flux leak-
age may be reduced by extending the end coils 302, 303
into the transverse coil region 408, 409. The turns
density per unit length near the center of the central
solenoid will typically be about 80% of the turns den-
30   sity near the end coils 302, 303 for improved field
linearity over a longer sample region.

The total number of turns in the end coils 302,
303 plus their extensions into the transverse region
408, 409 will typically be about one tenth of the total
35   turns per octopolar coil and is selected to minimize
axial leakage flux. The number of turns in the cross

-23-

coils **304, 305** or in the transverse saddle coils **401,
402,** whichever are used, is typically about one fifth
of the total number of turns and is selected primarily
to minimize transverse leakage flux for the system in
the absence of the passive shield.

The series inductance $L_1$ of the quadrant of octo-
polar coils is approximately

$$L_1 \approx \frac{\mu_0 n_1^2 r_i s}{h_i} , \qquad (22)$$

where $n_1$ is the number of turns on each octopolar coil
including the cross coils or Golay coils, and we have
assumed $h_i = 1.5 r_i$ and $s = 0.3 r_i$ in omitted second order
terms.

Most of the turns are linked by approximately
equal flux, $\phi_1 / n_C$, where $\phi_1$ is the total flux from the
quadrant through the z=0 plane. With the coils all
wired in series,

$$\phi_1 \approx \frac{L_1 I_1}{n_1} , \qquad (23)$$

where $I_1$ is the series current. For a parallel
arrangement, the inductance is decreased by $n_C^2$ and the
current is increased by $n_C$, requiring this factor to be
added to equation [23].

The average value of the z-component of the
magnetic field from one quadrant of coils in the x-y
plane at z=0, $<B_{z1}(0)>$, is easily estimated.

$$\langle B_{z1}(0) \rangle \approx \frac{\phi_1}{A_0} , \qquad (24)$$

$$A_0 \approx 2\pi r_i^2. \hspace{3cm} (25)$$

The radial distance $\epsilon$ between the magnetic shield and
the coils should be small compared to $s$, or leakage
flux is increased and $B_{z1}$ is decreased slightly,
5       particularly if the number of turns in the transverse
coils is not chosen to give optimum first-order
shielding.

A more sophisticated approach to calculating the
magnetic field, such as numerical integration of the
10      Biot-Savart law, is required to determine $B_{z1}$ as a
function of $x$.  However, a reasonable estimate of its
value near the x-y plane at $x=r_i$ is twice the average
value, and its value at $x=-r_i$ should be about 0.2 times
the average value.  (The field inside the central
15      solenoids 301 is approximately 10 times that of
equation [24].)

Figure 5 discloses the transverse gradient coil
system of the instant invention, which includes two
opposing quadrants 501, 502 of identical octopolar
20      coils with support structure.  The coils are energized
so that the average value of the axial component of the
magnetic field along the central axis is zero; the
average value over the central transverse plane is also
zero; the dipole moment of the total magnetic field
25      produced by the coil system is zero; the highly
localized fields result in a much smaller quadrupole
moment than for Golay coils of similar size; and there
are substantial octopole and higher multipole moments.

Eddy currents are induced in the passive
30      cylindrical gradient shield 308 such that the gradient
field is confined to the central region when the shield
thickness is greater than the skin depth $\delta$.  The
relatively low-level eddy currents induced by the

octopolar coils do not present major problems if the
shield rigidity and mass sufficiently limit coupling to
acoustic resonances.  It is primarily the acoustic
modes, rather than the directly induced eddy currents,
5    that have time constants long enough to cause image
artifacts that cannot be addressed by pulse shaping.
The main exception to this rule is the zero-order $B_z$ or
solenoidal component induced by imperfections in the
gradients, which has a decay time constant on the order
10   of $r_f t_g^{0.5}$ [$s^{0.5}$/m] for thick-walled copper cylinders.  But
this low-level homogeneous shift is easily nulled with
a low-power zero-order (quasi-Helmholtz) $B_z$ coil 503,
504 of radius less than that of the gradient shield 308
but larger than that of the internal rf shield 505.
15        The energy stored in the acoustic resonances in a
strong external magnetic field is responsible for the
persistence of the complex eddy currents via
microphonic interactions.  The eddy current time
constant may be decreased by using a high-resistivity
20   alloy for the shield such as austenitic (non-magnetic,
300-series) stainless steels (about 20% Cr, 10% Ni) or
by resistive damping as described later.  The acoustic
time constant is decreased by using a shield with high
velocity of sound, high stiffness, and high mechanical
25   loss factor.  Improved shielding may be obtained by
including a copper or aluminum cylinder, as the skin
depth in alloy AISI 304 (UNS S30400) at 20 Hz is about
100 mm while the skin depth in copper is only 15 mm.  A
copper cylinder 410, with 3 to 30 mm wall thickness, a
30   stainless steel cylinder 412, of 2 to 20 mm wall, and a
composite resin cylinder 411 therebetween, with resin
cylinder thickness less than one half of the total wall
thickness, provides a good balance of high stiffness,
high conductivity, low permeability, high acoustic
35   damping, and low cost.  Performance is a little better

with the copper or aluminum on the inside, but either
way provides an effective, passive shield.

The eddy current energy of the instant invention
is an order of magnitude lower than that of the
5    unshielded prior art, which greatly reduces the
gradient power demands imposed by multi-exponential
eddy current compensation techniques. Additional
active shielding, beyond optimization of the end coils
**302, 303** and transverse coils **401, 402**, is not
10   necessary.

The difference between the $B_z$ values at +x and 0,
according to the previous estimate, is about twice the
average value of equation [24]. With all the coils
electrically wired in series, the total inductance $L_T$ is
15   about $2L_1$ and the total current $I_T$ is $I_1$. The gradient
coefficient $\alpha$ is easily estimated.

$$\delta B = \frac{\beta L_T I_T}{n_i r_i^2}, \qquad (26)$$

$$\alpha = \frac{\delta B}{r_i l} = \frac{\beta L_T}{n_1 r_i^3}, \qquad (27)$$

Our estimate of the field slope implies that
20   $\beta \approx (2-.2)/4\pi \approx 0.14$. (Factors of $n_c$ are required to make
equations [22] through [28] valid for parallel
arrangements.) Substituting into equation [4] gives

$$\alpha = 2\frac{\beta \mu_0 n_1 s}{h_i r_i^2}, \qquad (28)$$

$$\eta_s = \frac{\beta^2 L_T}{\mu_0 n_1^2 r_i}, \tag{29}$$

$$\eta_s \approx 2 \frac{\beta^2 s}{h} \approx 0.005. \tag{30}$$

Equations [29] and [30] are dimensionless and
valid for either series or parallel arrangements. The
5  switching efficiency is clearly independent of $n_1$ and
$n_c$, and it is two to five times larger than for shielded
Golay-type coils of comparable $s/h$.

Another approach to understanding the reason
behind the higher switching efficiency of the octopolar
10  coil compared to the Golay coil is to note that only 5%
to 15% of the total conductor length is parallel to $B_z$.
By contrast, about 40% of the conductor length in the
Golay coils is parallel to $B_z$ with totally useless
magnetic field. This has not been perceived to be a
15  problem in the prior art because no forces are
generated by those conductors parallel to the external
field. However, the parallel conductors not only
generate harmful field components in the sample and in
the rf coils, they are responsible for torques and
20  hence the acoustic problems. Increasing $s$ and reducing
$h$ in equation [30] increases the switching efficiency
but the percentage of conductor length parallel to $B_z$
increases. The percentage of conductor length
substantially parallel to $B_z$ should be kept below 20%
25  for satisfactory control of transverse fields and
acoustic problems. Decreasing $h$ has the advantage of
limiting the field of view and thus reducing the
biological hazards from large switching fields.

It should be noted that decreasing the axial field
30  of view by 30% would seldom be a disadvantage, as the

50-ms snapshots possible with EPI would permit the
patient to be smoothly conveyed through the imaging
zone with little difficulty in treating motion-related
artifacts.  Proper signal averaging and registration of
successive images could readily be achieved.

As the prior art has often been concerned with
reducing inductance, we note that the octopolar coils
can achieve two orders-of-magnitude lower inductance
than Golay-type coils before shielding problems become
significant.  The total number of turns can be as small
as 40 per octopolar coil without excessive flux leak-
age.  The minimum inductance is thus about $2\mu_0 r_i$, or
under 1 $\mu$H for a whole-body parallel octopolar coil
system, but the performance per cost of the driver is
usually best for 0.2 to 1 mH.

Orthogonality between the three axes should be
within 0.01% for EPI.  Achieving this degree of ortho-
gonality directly is beyond reasonable manufacturing
tolerances, but an external variable coupling (cross-
term) circuit at the input of the gradient drivers can
be used to null residual magnetic couplings.  Maintain-
ing magnetic orthogonality over a typical range of 5 Hz
to 5 kHz requires a high degree of precision in the
symmetry of the passive gradient shield, the internal
rf shield, and the rf coil.   Electric field interac-
tions between the axes can easily be made smaller than
0.05% by using balanced coil drivers with low induc-
tance gradient systems (below 1 mH).  Winding each
quadrant in a series-parallel fashion that leaves the
low-voltage points at the edges of the quadrants and
the high-voltage points at the centers of the quadrants
makes it easy to achieve another order of magnitude
reduction in electric field coupling.  A typical
winding would be 100 to 200 turns per octopolar coil,
with half of the octopolar coils per quadrant connected
in series and paralleled with the other half.

-29-

As can be appreciated by one experienced in the
manufacture of Golay coilforms and the winding of Golay
coils, the solenoidal octopolar coils are much easier
to produce, especially with the high degree of accuracy
5   necessary for precise shielding, axis orthogonality,
and low homogeneous shift.

The DC resistance of the series-connected
octopolar gradient system is easily shown to be

$$R_E \approx 15 \frac{n_1^2 \rho r_i}{c_t h_i} , \qquad (31)$$

10  where $\rho$ is the conductivity of the wire and $c_t$ is the
conductor thickness in the coils, for $c_t$ less than the
skin depth.  Substituting equations [28] and [31] into
equation [10] gives the following low frequency
efficiency:
15

$$\eta_L \approx \frac{\beta^2 \sqrt{\omega} \mu_0 c_t s^2}{5 h_i r_i \rho} . \qquad (32)$$

At 100 Hz, the above expression simplifies to
approximately $0.3 c_t / r_i$ for the previous conditions.  For
$c_t$=6 mm and $r_i$=300 mm, this evaluates to 0.005 and is an
20  order of magnitude larger than for typical prior-art,
whole-body MRI transverse gradients.  The figure of
merit governing power dissipation during EPI is $\eta_s Q$.
For the above solenoidal octopolar coil geometry,

$$Q \approx 0.25 \frac{s}{\delta} , \qquad (33)$$

25  where the skin depth $\delta$ is assumed to be small compared
to $c_t$, and other losses are small.  For the previous
example, the Q is about 15 at 1600 Hz since $\delta$=1.6 mm.

The coefficient in equation [33] varies between 0.1 and 0.4 for shielded Golay coils, depending primarily on the conductor surface area and the degree of linearization.

5        Another qualitative method of evaluating coil shielding problems is to measure the change in inductance when a passive shield is added. For the unshielded Golay coils, a passive shield with inner radius $1.3r_f$ typically reduces the inductance by 25%.

10     For the shielded Golay coils, a passive shield at radial distance $\epsilon$ from the shield coil, where $\epsilon=0.03r_i$, may reduce the inductance by under 0.5% for high-inductance coils, but several percent is more typical for low-inductance coils. For the octopolar coils

15     without additional shielding coils, the passive shield at $\epsilon=0.03r_i$ reduces the inductance by several percent. The addition of low-power Golay shielding coils can reduce the effect of the passive shield on inductance change by another order of magnitude.

20        Finally, we note that linearity over the sphere of radius $r_i$ for the conditions previously assumed is easily better than ±30%. With proper control of winding densities, especially in the solenoidal coils extending into the cross coil regions, linearity can be

25     better than ±20%. Where space permits, increasing $s/r_f$ improves linearity as well as efficiencies. Optimized winding densities that balance efficiencies, flux shielding, and linearity may be determined by prior-art iterative techniques using the above equations and

30     standard numerical integration of the Biot-Savart law.

Figure 6 discloses a shielded axial gradient coil system with concentric support members 601. It is important that the z-gradient coils 602 and z-gradient shield coils 603 be wound on coilforms of high-modulus

35     materials and rigidly joined through the concentric support members 601 to minimize their motion-related

artifacts and acoustic noise.  One of the stiffest
thermoplastics readily available is nylon 6/6 rein-
forced with 60% long glass fiber.  Further increase in
modulus may be achieved by using a high-strength
5    alumina-silica-boria ceramic fiber such as 3M's Nextel
480, or zirconia fibers, or alumina fibers instead of
glass fibers.  The low shear strength of such fibers
results in low impact strength, which may facilitate
machining.  Improved impact strength can be achieved by
10   using a thermoset resin such as polyester or epoxy with
a room-temperature cure process allowing high-modulus
carbon fibers to be substituted for a fraction of the
ceramic fibers.  Carbon fiber content must be kept
below 15% or electrical conductivity becomes large
15   enough to cause excessive eddy current losses.  Low-
temperature cures are required because of the differ-
ential thermal expansion between carbon and ceramic
fibers which places the ceramic fibers under tensile
stress upon cooling.  A preferred composite would
20   include at least 5% carbon fibers and at least 25%
ceramic fibers by mass.

For best results, the wires should be securely
bonded to the forms with epoxy containing at least 5%
carbon fiber to improve both thermal conductivity and
25   modulus.  At least 10% other non-conductive, high-
modulus fiber having elastic modulus greater than 60
GPa, such as ceramic fiber or glass fiber, is bene-
ficial for further increase in modulus.

Figure 7 discloses a quadrant of an axial cross
30   section of the typical x-y-z gradient system of the
instant invention, which is symmetric with respect to a
180° rotation about the z-axis and symmetric with
respect to a reflection through the x-y plane.  The
solenoidal coilforms 405 function as concentric support
35   members and support the central solenoids 301 and
transverse saddle coils 401.  Z-gradient motion is

reduced by bonding the outside of the z-gradient coil-
form 704 to the inside of each of octopolar coils 405
and bonding the inside of the z-shielding coilform 705
to the outside of each of the octopolar coils 405. The

5    radial forces from the axial gradient coils 706, 707
are opposite those of the axial shielding coils 708,
709, 710 and coupled through the highly rigid sole-
noidal coilforms. As a result, only the residual net
force, which is about half of the radial force of the

10   gradient coils, produces significant motion.

The external passive gradient shield 701, 702,
703, corresponding to shield 308 substantially elimi-
nates eddy current effects (cryogen boiling and field
distortions) in the magnet. It includes copper cylin-

15   der 410, resin cylinder 702, and stainless steel
cylinder 703, corresponding to the above mentioned 410,
411, and 412.

A low-power quasi-Helmholtz zero-order shim coil
503 may be added for real-time cancellation of the

20   minute solenoidal eddy currents caused by imperfections
in the gradients. Placing this $B_0$ correction coil
inside the passive gradient shield 308 is far more
effective than attempting to adjust the current in the
main magnet $B_0$ windings to cancel offsets from eddy

25   currents, as suggested by Kondo in U.S. Patent No.
5,055,789, or by using the standard $B_0$ shim coil pro-
vided inside the magnet cryostat. A zero-order shield
coil 712 is added to simplify the time dependence of
the offset correction. The axial location of the

30   zero-order shim coil 503 and its symmetric counterpart
are centered approximately at $\pm z=0.55 r$, to improve
homogeneity in the presence of the zero-order shield
coil 712. The x-y-z gradient coils may be used for
cancellation of first-order gradients from eddy cur-

35   rents by pulse shaping as described by Van Vaals et al.

Second-order, time-dependent correction to $B_z$ is
also beneficial. An orthogonal $B_z^2$ shim coil could
consist of the second order shim coils 713, 714. Coil
713 is centered about the origin and contains $I_2$
5        amp-turns. Coil 714 and its symmetric counterpart
could be centered at $\pm z \approx 1.1 r_f$ and each contain $0.5 I_2$
negative amp-turns for minimum dipole moment.
Second-order shield coils 715, 716 are added to sim-
plify time dependence. Fine conductors are sufficient
10       for the zero-order and second-order shim and shield
coils, as they are required only to generate fields
less than 0.01% of $B_0$, while the x-y-z gradient fields
may exceed 10% of $B_0$. Higher-order, time-dependent,
shielded shim coils would seldom be beneficial owing to
15       the extremely short time constants of the higher-order
eddy current modes.

The inside of the gradient coilform must be lined
with an rf noise shield 717, 718, for optimum sensi-
tivity and rf tuning stability. Pure copper or silver
20       foil, about 0.1-mm thick, is sufficient for rf noise
shielding above 12 MHz. Eddy current problems, except
for zero-order $B_z$, are not too significant at this foil
thickness, and microphonic problems are controlled by
securely bonding the foil to the rigid coilform. An
25       improvement in gradient efficiency at higher switching
frequencies and a reduction of eddy currents may be
obtained by using a copper alloy foil with high elec-
trical resistivity, such as high-silicon bronze alloy
C65500, where $\rho \approx 250$ nΩm, or type 330 stainless steel,
30       where $\rho \approx 1000$ nΩm, compared to 17 nΩm for copper, but
other alloys with resistivity above 100 nΩm would also
be quite advantageous compared to copper for rf noise
shielding and eddy current damping - i.e., the high-
resistivity foil is effectively a shunt resistor
35       inductively coupled into the eddy current field. The
foil thickness may be increased by the square root of

the increase in resistivity to typically 0.2 to 1-mm
for equivalent noise shielding. The rf Q of small MRI
surface coils would not be significantly affected by
the high-resistivity noise shield, and a 0.01-mm to
5   0.03-mm silver plate on the inside surface of the noise
shield is sufficient to maintain high Q in large rf
coils. The increased inside diameter of the rf shield
in the central region 717 compared to the end region
718 allows maximum rf performance by providing the
10   largest possible volume outside the rf coil 307 for rf
flux return (effectively increasing the rf filling
factor by reducing the external flux density and hence
the integral of $B_1^2$ over the external volume) while
making more space available for support of the axial
15   gradient coils 706, 707.

It is in fact possible to eliminate all saddle
coils, cross coils, shim coils, and axial gradient
coils and simply utilize the axial solenoids to
generate transverse gradients when $s/h_t$ is large, the
20   passive shield is long, and end coils 302 are used to
generate an axial quadrupolar field. The eddy currents
then induced in the passive shield produce the desired
octopolar field. An even number of solenoidal-like
axial coils is required - preferably 4n, where n is an
25   integer. The solenoid cross sections may be round,
trapezoidal, or elliptical. They are positioned such
that the distance between the central z-axis and each
axial coil axis is greater than the major diameter of
the solenoids. Opposed currents are applied to the
30   solenoids to generate a transverse gradient.

Figure 8 is a schematic representation identifying
those portions of the MRI system most directly related
to the instant invention. The superconducting magnet
309 and cryoshims are fully persistent, requiring no
35   real-time control because the highly localized flux
from the actively shielded gradient system 801 in

cooperation with the passive shield **308** effectively
eliminates eddy currents in the magnet. The frequency-
encoding gradient driver **802** would typically be rated
at several hundred kilowatts, DC to 20 kHz, and its
5    gradient coil may be tuned to 1 to 2 kHz. The other
gradient drivers **803, 804** would typically be rated at
five kilowatts, but hundreds of kilowatts could be used
for greater flexibility. Much less power is required
for the optional transverse shield-coil drivers **805,**
10   **806** and axial shield driver **807**. The real-time offset
shim driver **808** and real-time $z^2$ shim driver **809** would
typically be ultra-quiet DC-50 kHz amplifiers rated
less than 100 W continuous. A high-resistivity noise
shield **810** isolates the tuned rf coil **307** from the
15   gradient noise and helps damp eddy currents. The
nuclei in the sample are magnetized by rf pulses at the
mean Larmor frequency from a high-power rf amplifier
**811**, and the precession signals are amplified by
low-noise preamp **812** and processed by the computer **813**.
20        Figure 9 discloses a quadrant of a longitudinal
cross section of a c-coil embodiment of the instant
invention for the generation of transverse gradients.
Non-ferromagnetic c-coils **900** rather than solenoids,
are symmetrically distributed around the inside peri-
25   meter of a passive shield **308** inside the bore of a
superconducting magnet in a fashion similar to that
depicted in Figures 4 and 5. The passive shield **308**
prevents significant interaction with the magnet, and
eddy current effects may be canceled with gradient
30   pulse shaping according to the prior art and time-
dependent zero-order and second-order shim coils as
described previously. Partial-toroidal section **902** at
each end of a central solenoidal section **901** reduces
flux leakage. Performance is substantially better than
35   prior art transverse gradient coils with respect to

acoustic noise and manufacturability but efficiencies
and linearity are inferior.

Figure 10 discloses a quadrant of a longitudinal
cross section of a u-coil embodiment of the instant
5    invention for the generation of transverse gradients.
U-coils 1000, comprising an axial central solenoidal
section 1002 and a transverse section 1001 at each end,
are symmetrically distributed around the inside peri-
meter of a passive shield 308 inside the bore of a
10   superconducting magnet in a fashion similar to that
depicted in Figures 4 and 5. Performance is somewhat
inferior to that of the octopolar coils of Figure 4 but
generally better than that of the c-coils of Figure 9.

Turning now to Fig. 11, there is shown an axial
15   end view of the structure of Fig. 5. As was mentioned
above in connection with Fig. 7, the solenoidal coil-
forms may be in cross section round, trapezoidal, or
elliptical. Fig. 11 shows the trapezoidal configura-
tion, with trapezoidally shaped solenoid coilforms 405
20   which offers higher gradient coefficient as the ratio
of the mean distances from the sample to the outer and
inner current elements responsible for the gradient has
increased. Also, the space available for external flux
has increased, thus reducing the energy in the external
25   field. The cross section is not a true trapezoid, as
the edges are radiused and the flats are slightly
convex to facilitate coil winding.

As was described above in connection with Fig. 7,
one embodiment of the solenoid is to have the trans-
30   verse coil 401 interleaved with a portion of the
central solenoid 301 and interleaved with a portion of
the end coil 302. As mentioned above, this interleav-
ing reduces transverse and axial flux leakage. The
central solenoid is partitioned into 2n+1 parts, and
35   the end coil is partitioned into n+1 parts, where n=1.

However, those skilled in the art will appreciate
that a slightly more complex solenoid configuration
would reduce flux leakage still further. Fig. 12
illustrates at (b) such an alternative embodiment for a

5    coil assembly where n=2 for the central solenoid but
n=1 for the end coil. At (a) is seen a side view of a
coilform 405 such as appears in Fig. 7. As described
previously, end coil 302 has been partitioned physi-
cally into coils 302 and 408, and central solenoid 301

10   has been partitioned physically into coils 301 and 406,
while transverse coil 401 is interleaved, passing for
example between coils 302 and 408, and between coils
301 and 406. At (b) is seen a corresponding side view
of the more complex solenoid configuration. End coil

15   302 has been partitioned physically into coils 302,
408, and central solenoid 301 has been partitioned
physically into coils 301, 406a, and 406b. Transverse
coil 401 is partitioned into coils 401a and 401b. As
shown at (b), transverse coil 401a is interleaved,

20   passing for example between coils 302 and 408, and
between coils 301 and 406a. Transverse coil 401b is
interleaved, passing for example between coils 408, and
between coils 406a and 406b. Thus the central coil is
in five parts, and each end coil is in two parts.

25   Many variants are possible without departing from
the basic principle of interleaving. For example, for
n=2 for the end coil, coil 408 in the structure at (b)
would be divided into two parts, with an upper portion
as shown and a lower portion inside coil 401b adjacent

30   to coil 406b. Alternatively, with n=3 for the central
solenoid, coil 301 in the structure at (b) would be
divided again, with another cross coil 401c.

Still further variants may be found in interleav-
ing with finer structure, for example, where n has

35   values higher than 2. Flux leakage would be reduced

still further, though with the tradeoff of a more
complex structure for the coil.

It will be appreciated that the reflective
symmetry requirement for the solenoid entails that
5   central solenoid 301 is partitioned into an odd number
of coils, namely 2n+1.

Figure 13 illustrates an alternative embodiment
for a coil assembly in accordance with the invention
wherein an octapolar field is obtained without the use
10  of radially aligned cross coils.  The solenoidal-like
windings are inclined at pronounced, symmetric angles
at opposite ends 1302, 1303 of the central solenoid
1301.  Orthogonal fields are produced by the inclined
end coils 1304, 1305.  These octopolar coils are
15  distributed around the perimeter of the bore of the
superconducting magnet in the manner illustrated in
Figures 4 and 5 for octopolar solenoids having radially
aligned cross coils.

Although this invention has been described herein
20  with reference to specific embodiments, it will be
recognized that changes and modifications may be made
without departing from the spirit of the present
invention.  All such modifications and changes are
intended to be included within the scope of the
25  following claims.

<u>Claims</u>

1  1.   A non-ferromagnetic transverse gradient coil
2        system having a central axis, said system
3        comprising:
4            an even number of solenoidal-like central
5        axial coils having a major diameter wound on rigid
6        coilforms having axial coil axes parallel to said
7        central axis and positioned such that the distance
8        between said central axis and each said axial coil
9        axis is greater than the major diameter of said
10       axial coils, the coils arranged in two groups, the
11       groups substantially symmetrical to each other
12       with respect to 180° rotation about the central
13       axis, the coils being substantially symmetrical
14       with respect to reflection through a plane
15       perpendicular to said central axis.

1  2.   The coil system of claim 1 wherein each of said
2        axial coils further characterized by having turns
3        density at symmetrical non-central locations
4        greater than the turns density near its center.

1  3.   The coil system of claim 1 wherein each of the
2        groups of coils further comprises a pair of saddle
3        coils symmetrically disposed one near a first end
4        of the axial coils and the other near the other
5        end of the axial coils, said saddle coils having
6        axes aligned substantially radially from said
7        central axis.

1  4.   The coil system of claim 1 in which each axial
2        coil further comprises end coils coaxial with the
3        central coil thereof and symmetrically secured
4        beyond the end of said central coil.

1  5.  The coil system of claim 1 further comprising a
2      metallic shield cylinder having electrical conduc-
3      tivity less than 30 nano-ohm-meters symmetrically
4      surrounding said coil system.


1  6.  The coil system of claim 1 in which said rigid
2      coilforms are made from a nonmetallic material
3      have elastic modulus greater than 12 GPa and
4      density greater than 2 g/cm³.


1  7.  The coil system of claim 1 in which said central
2      coils are further characterized by having windings
3      inclined with respect to the coil axis.


1  8.  The coil system of claim 1 in which said rigid
2      coilforms have substantially trapezoidal cross-
3      section.


1  9.  The coil system of claim 1 further comprising a
2      plurality of cross coils disposed at each end of
3      said central coils, said cross coils having axes
4      aligned substantially radially.


1  10.  The coil system of claim 9 in which said axial
2      coils generate a transverse gradient field and in
3      which said saddle coils, when energized, generate
4      a transverse quadrupolar field such that said
5      transverse gradient field is increased in said
6      central region.


1  11.  The coil system of claim 10 in which said end
2      coils and said central coils, when energized,
3      generate a magnetic field with a substantial axial
4      quadrupolar component.

1    12.   The coil system of claim 1 in which said rigid
2          coilforms have substantially round cross-section.


1    13.   The coil system of claim 1 in which said coilform
2          made from a material selected from the set
3          consisting of alumina, silicon nitride, zirconia,
4          alumina-silica-boria glasses, borosilicate
5          glasses, machinable glasses, plastic composites
6          having at least 10% carbon fiber content, plastic
7          composites having more than 25% ceramic fiber
8          content, and plastic composites having density
9          greater than 2.0 g/cm$^3$.


1    14.   An x-y gradient coil system comprising first and
2          second non-ferromagnetic transverse gradient coil
3          systems, each transverse gradient coil system
4          being substantially symmetrical with respect to
5          180° rotation about a central axis and substan-
6          tially symmetrical with respect to reflection
7          through a plane perpendicular to said central
8          axis, each said transverse gradient coil system
9          comprising an even number of solenoidal-like
10         central axial coils having a major diameter wound
11         on rigid coilforms having axial coil axes parallel
12         to said central axis and positioned such that the
13         distance between said central axis and each said
14         axial coil axis is greater than the major diameter
15         of said axial coils, each of said axial coils
16         further characterized by having turns density at
17         symmetrical non-central locations greater than the
18         turns density near its center, the central axes of
19         the transverse gradient coil systems being coinci-
20         dent, the transverse gradient coil systems being
21         oriented orthogonally to each other, whereby said
22         x-y coil system is capable of producing transverse

23    gradients in the central axial field in two
24    orthogonal directions.


1    15.    The coil system of claim 14 in which said central
2           axial coils are substantially round in cross
3           section.


1    16.    The coil system of claim 14 in which said central
2           axial coils are substantially trapezoidal in cross
3           section.


1    17.    A gradient coil system for use in magnetic
2           resonance imaging employing a superconducting
3           magnet to establish a magnetic field $B_z$, said coil
4           system comprising:
5                current conducting elements disposed to
6           generate a transverse gradient in $B_z$, said
7           conducting elements arranged such that they are
8           substantially nonparallel to $B_z$ over more than 80%
9           of their total length;
10               a rigid form to support said conducting
11          elements;   and
12               said conducting elements further comprising:
13               a plurality of loops having dipole moment
14          parallel to $B_z$;
15               a plurality of loops having dipole moment
16          perpendicular to $B_z$;
17               said loops arranged substantially symmetri-
18          cally with respect to a 180° rotation about the z
19          axis and substantially symmetrically with respect
20          to a reflection through a plane perpendicular to
21          said axis.


1    18.    The coil system of claim 17 in which said loops
2           having dipole moment parallel to $B_z$ are
3           substantially round.

1   19.   The coil system of claim 17 in which said loops
2        having dipole moment parallel to $B_z$ are
3        substantially trapezoidal.

1   20.   A non-ferromagnetic elongate U-coil for producing
2        an external localized flux region, said U-coil
3        comprising:
4           a central substantially solenoidal coil wound
5        on a coilform of length $h_s$ and major diameter $d_s$
6        and having a mean first axis of symmetry;
7           two transverse coils, one disposed at each
8        end of said central solenoidal coil, having axes
9        perpendicular to said first axis, and having
10       outside diameter $d_T$ and axial length $h_T$ such that
11       $h_T$ is less than $d_s$.

1   21.   The U-coil of claim 20 in which each said trans-
2        verse coil comprises a cross coil, each said cross
3        coil wound on the coilform.

1   22.   the U-coil of claim 20 in which each said trans-
2        verse coil comprises a saddle coil portion, said
3        saddle coil portion comprising conductors threaded
4        through transverse holes in the coilform.

1   23.   The U-coil of claim 20 in which said central
2        solenoidal coil is substantially round in cross
3        section.

1   24.   The U-coil of claim 20 in which said central
2        solenoidal coil is substantially trapezoidal in
3        cross section.

4   25.   The U-coil of claim 20 in which said coilform is
5        made from a material selected from the set

6       consisting of alumina, silicon nitride, zirconia,
7       alumina-silica-boria glasses, borosilicate
8       glasses, machinable glasses, plastic composites
9       having at least 10% carbon fiber content, plastic
10      composites having more than 25% ceramic fiber
11      content, and plastic composites having density
12      greater than 2.0 g/cm$^3$.

1    26.  A gradient coil system comprising a plurality of
2        U-coils, each U-coil comprising a central substan-
3        tially solenoidal coil wound on a coilform of
4        length $h_s$ and major diameter $d_s$ and having a mean
5        first axis of symmetry, and two transverse coils,
6        one disposed at each end of said central sole-
7        noidal coil, having axes perpendicular to said
8        first axis, and having outside diameter $d_T$ and
9        axial length $h_T$ such that $h_T$ is less than $d_s$,
10           said U-coils distributed about a central axis
11       in two groups, the groups disposed substantially
12       symmetrically with respect to a 180-degree
13       rotation about said central axis and substantially
14       symmetrical with respect to a reflection through a
15       plane perpendicular to said central axis.

1    27.  The system of claim 26 in which each said trans-
2        verse coil comprises a cross coil, each said cross
3        coil wound on a respective solenoidal coilform.

1    28.  The system of claim 26 in which each said trans-
2        verse coil comprises a saddle coil portion, said
3        saddle coil portion comprising conductors threaded
4        through transverse holes in the solenoidal coil-
5        form;  the saddle coil portions together defining
6        transverse saddle coils threaded through the
7        transverse holes.

1   29.   The system of claim 26 in which each said central
2         solenoidal coil is substantially round in cross
3         section.

1   30.   The system of claim 26 in which each said central
2         solenoidal coil is substantially trapezoidal in
3         cross section.

1   31.   A non-ferromagnetic elongate c-coil for producing
2         an external localized flux region, said c-coil
3         comprising:
4             a central substantially solenoidal coil
5         having an axis, said coil of axial length $h_s$ and
6         major diameter $d_s$ wound on a rigid solenoidal
7         coilform for which $h_s$ is greater than $d_s$;
8             two partial-toroidal coils, each wound on a
9         rigid partial-toroidal coilform, said partial-
10        toroidal coils disposed symmetrically in a first
11        plane at respective ends of said solenoidal coil;
12        and
13            a tapered section connecting said partial-
14        toroidal coilform to said solenoidal coilform,
15        said tapered section being inclined at a small
16        acute angle in said first plane with respect to
17        said axis of said solenoidal coil;
18            said c-coil further characterized by being
19        substantially symmetrical with respect to a
20        reflection through a second plane perpendicular to
21        the axis of said solenoidal coil.

1   32.   The c-coil of claim 31 in which said solenoidal
2         coilform in made from a nonmetallic material with
3         elastic modulus greater than 12 GPa.

1   33.   The c-coil of claim 31 in which said central
2         substantially solenoidal coil is substantially
3         round in cross section.


1   34.   The c-coil of claim 31 in which said central
2         substantially solenoidal coil is substantially
3         trapezoidal in cross section.


1   35.   A transverse gradient coil system comprising a
2         plurality of c-coils, each c-coil comprising:
3             a central substantially solenoidal coil
4         having an axis, said coil of axial length $h_s$ and
5         major diameter $d_s$ wound on a rigid solenoidal
6         coilform for which $h_s$ is greater than $d_s$;
7             two partial-toroidal coils, each wound on a
8         rigid partial-toroidal coilform, said partial-
9         toroidal coils disposed symmetrically in a first
10        plane at respective ends of said solenoidal coil;
11        and
12            a tapered section connecting said partial-
13        toroidal coilform to said solenoidal coilform,
14        said tapered section being inclined at a small
15        acute angle in said first plane with respect to
16        said axis of said solenoidal coil;
17            said c-coil further characterized by being
18        substantially symmetrical with respect to a
19        reflection through a second plane perpendicular to
20        the axis of said solenoidal coil;
21            said c-coils distributed about a central axis
22        so as to be geometrically substantially
23        symmetrical with respect to a 180° rotation about
24        said central axis and having said second planes
25        coincident.

1   36.  The system of claim 35 in which each said central
2        solenoidal coil is substantially round in cross
3        section.

1   37.  The system of claim 35 in which each said central
2        solenoidal coil is substantially trapezoidal in
3        cross section.

1   38.  An x-y gradient coil system comprising first and
2   second transverse gradient coil systems, each
3   transverse gradient coil system comprising a plurality
4   of c-coils, each c-coil comprising:
5              a central substantially solenoidal coil
6        having an axis, said coil of axial length $h_s$ and
7        major diameter $d_s$ wound on a rigid solenoidal
8        coilform for which $h_s$ is greater than $d_s$;
9              two partial-toroidal coils, each wound on a
10       rigid partial-toroidal coilform, said partial-
11       toroidal coils disposed symmetrically in a first
12       plane at respective ends of said solenoidal coil;
13       and
14             a tapered section connecting said partial-
15       toroidal coilform to said solenoidal coilform,
16       said tapered section being inclined at a small
17       acute angle in said first plane with respect to
18       said axis of said solenoidal coil;
19             said c-coil further characterized by being
20       substantially symmetrical with respect to a
21       reflection through a second plane perpendicular to
22       the axis of said solenoidal coil;
23             said c-coils distributed about a central axis
24       so as to be geometrically substantially
25       symmetrical with respect to a 180° rotation about
26       said central axis and having said second planes
27       coincident;

28          the first and second transverse gradient coil
29      systems disposed so that said central axes and
30      said second planes are coincident, the gradient
31      coil systems disposed orthogonally to each other,
32      whereby said x-y coil system produces transverse
33      gradients in the central axial field in two
34      orthogonal directions.


1    39.  The system of claim 38 in which each said central
2         solenoidal coil is substantially round in cross
3         section.


1    40.  The system of claim 38 in which each said central
2         solenoidal coil is substantially trapezoidal in
3         cross section.


1    41.  A passive cylindrical RF shield of the type for
2         use in magnetic resonance imaging employing a
3         superconducting magnet to establish a magnetic
4         field $B_z$, said shield comprising:
5              a nonmagnetic metal alloy foil having bulk
6         resistivity greater than 100 nano-ohm-meters and a
7         plating less than 0.03 mm thick on one side of
8         said foil, said plating being either copper or
9         silver, said foil having thickness between 0.2 mm
10        and 1 mm, and said shield symmetrical about the z
11        axis and symmetrical with respect to a reflection
12        through a plane perpendicular to said axis.


1    42.  An RF shield for a gradient coil system for use in
2         magnetic resonance imaging employing a
3         superconducting magnet to establish a magnetic
4         field $B_z$, said coil system comprising a plurality
5         of current conducting elements disposed to
6         generate a transverse gradient in $B_z$, said element
7         disposed substantially symmetrically with respect

| | | |
|---|---|---|
| 8 | | to a 180° rotation about the z axis and |
| 9 | | substantially symmetrically with respect to a |
| 10 | | reflection through a plane perpendicular to said |
| 11 | | axis, said elements disposed at minimum distance |
| 12 | | $r_{min}$ from said axis and maximum distance $r_{max}$ from |
| 13 | | said axis, said RF shield comprising: |
| 14 | | a cylindrical foil with radius larger than $r_{min}$ |
| 15 | | but smaller than $r_{max}$ substantially centered within |
| 16 | | said system. |
| 1 | 43. | A passive cylindrical gradient shield for use in |
| 2 | | magnetic resonance imaging employing a |
| 3 | | superconducting magnet to establish a magnetic |
| 4. | | field $B_z$, said shield symmetrical about the z axis |
| 5 | | and symmetrical with respect to a reflection |
| 6 | | through a plane perpendicular to said axis; |
| 7 | | said shield comprising an inner metallic |
| 8 | | cylinder, an outer metallic cylinder, and a resin |
| 9 | | cylinder bonded therebetween; |
| 10 | | said metallic cylinders having wall thickness |
| 11 | | greater than 2 mm and less than 40 mm; |
| 12 | | said resin cylinder having wall thickness |
| 13 | | less than one half of the total wall thickness of |
| 14 | | said shield; |
| 15 | | one of said metallic cylinders being an alloy |
| 16 | | having electrical resistivity less than 30 nano- |
| 17 | | ohm-meters and the other of said metallic |
| 18 | | cylinders being an austenitic Cr-Ni-Fe alloy. |
| 1 | 44. | A gradient coil system for use in magnetic |
| 2 | | resonance imaging employing a superconducting |
| 3 | | magnet to establish a magnetic field $B_z$, said |
| 4 | | system substantially symmetrical with respect to a |
| 5 | | 180° rotation about the z axis and substantially |
| 6 | | symmetrical with respect to a reflection through a |

|    |     |                                                        |
|----|-----|---------------------------------------------------------|
| 7  |     | plane perpendicular to said axis;  said coil            |
| 8  |     | system comprising:                                      |
| 9  |     | a gradient assembly comprising:                         |
| 10 |     | gradient coils for generating gradients in $B_z$;       |
| 11 |     | and                                                     |
| 12 |     | a rigid form to support said coils;                     |
| 13 |     | a conductive passive gradient shield with               |
| 14 |     | diameter greater than the outside diameter of said      |
| 15 |     | gradient assembly;                                      |
| 16 |     | a conductive RF shield with diameter less               |
| 17 |     | than the inside diameter of said gradient               |
| 18 |     | assembly; and                                           |
| 19 |     | an axially aligned zero-order $B_z$ shim coil           |
| 20 |     | with diameter less than that of said passive.           |
| 21 |     | shield but greater than that of said RF shield.         |
|    |     |                                                         |
| 1  | 45. | A gradient coil system for use in magnetic              |
| 2  |     | resonance imaging employing a superconducting           |
| 3  |     | magnet to establish a magnetic field $B_z$, said        |
| 4  |     | system substantially symmetrical with respect to a      |
| 5  |     | 180° rotation about the z axis and substantially        |
| 6  |     | symmetrical with respect to a reflection through a      |
| 7  |     | plane perpendicular to said axis;  said coil            |
| 8  |     | system comprising:                                      |
| 9  |     | a gradient assembly comprising:                         |
| 10 |     | gradient coils for generating gradients in $B_z$;       |
| 11 |     | and                                                     |
| 12 |     | a rigid form to support said coils;                     |
| 13 |     | a conductive passive gradient shield with               |
| 14 |     | diameter greater than the outside diameter of said      |
| 15 |     | gradient assembly;                                      |
| 16 |     | a conductive RF shield with diameter less               |
| 17 |     | than the inside diameter of said gradient               |
| 18 |     | assembly; and                                           |
| 19 |     | an axially aligned second-order shielded $B_z$          |
| 20 |     | shim coil with diameter less than that of said          |

21      passive shield but greater than that of said RF
22      shield.


 1   46.  A gradient coil system for use in magnetic
 2        resonance imaging employing a superconducting
 3        magnet to establish a magnetic field $B_z$, said coil
 4        system comprising:
 5            gradient coils for generating an axial
 6        gradient $dB_z/dz$ disposed on a first cylinder;
 7            shielding coils disposed on a second cylinder
 8        of radius larger than that of first said cylinder;
 9        and
10            at least four rigid support members disposed
11        axially in the radial space between said first and
12        second cylinders and bonded to said first and
13        second cylinders to permit rigid transfer of
14        radial forces.


 1   47.  A gradient coil system for use in magnetic
 2        resonance imaging employing a superconducting
 3        magnet to establish a magnetic field $B_z$, said
 4        elements substantially symmetrical with respect to
 5        a 180° rotation about the z axis and substantially
 6        symmetrical with respect to a reflection through a
 7        plane perpendicular to said axis;  said coil
 8        system comprising:
 9            current conducting elements for generating a
10        transverse gradient in $B_z$;
11            a rigid form to support said conducting
12        elements; and
13            a thermoset resin bonding said conducting
14        elements to said form;
15            said resin containing at least 5% carbon
16        fibers and at least 10% nonconductive fiber by
17        mass; and

18          said nonconductive fiber having modulus
19      greater than 60 GPa.


1   48.  A non-ferromagnetic elongate coil for producing an
2        external localized flux region, said coil
3        comprising:
4            a central substantially solenoidal coil wound
5        on a coilform of length $h_s$ and major diameter $d_s$
6        and having a mean first axis of symmetry;
7            two transverse coils, one disposed at each
8        end of said central solenoidal coil, having axes
9        perpendicular to said first axis, and having
10       outside diameter $d_T$ and axial length $h_T$ such that
11       $h_T$ is less than $d_s$;
12           a portion of the turns of each of the
13       transverse coils interleaved with a portion of the
14       turns of the central substantially solenoidal
15       coil.


1   49.  The coil of claim 48 in which each said transverse
2        coil comprises a cross coil, each said cross coil
3        wound on a respective solenoidal coilform.


1   50.  The coil of claim 48 in which each said transverse
2        coil comprises a saddle coil portion, said saddle
3        coil portion comprising conductors threaded
4        through transverse holes in the solenoidal
5        coilform.


1   51.  The coil of claim 48 in which said central
2        solenoidal coil is substantially round in cross
3        section.


1   52.  The coil of claim 48 in which said central
2        solenoidal coil is substantially trapezoidal in
3        cross section.

1    53.    The coil of claim 48 in which said coilform is
2           made from a material selected from the set
3           consisting of alumina, silicon nitride, zirconia,
4           alumina-silica-boria glasses, borosilicate
5           glasses, machinable glasses, plastic composites
6           having at least 10% carbon fiber content, plastic
7           composites having more than 25% ceramic fiber
8           content, and plastic composites having density
9           greater than 2.0 g/cm$^3$.

1    54.    The coil of claim 48 in which the central
2           substantially solenoidal coil is partitioned into
3           top, middle, and bottom portions, a first of the
4           transverse coils is interleaved with the top
5           portion, and the other of the transverse coils is
6           interleaved with the bottom portion.

1    55.    The coil of claim 48 in which the central
2           substantially solenoidal coil is partitioned into
3           first, second, third, fourth, and fifth portions,
4           and each of the transverse coils is partitioned
5           into outer and inner portions, the outer portions
6           surrounding the respective inner portions;  the
7           outer portion of a first of the transverse coils
8           interleaved with the first and second portions,
9           the outer portion of the other of the transverse
10          coils interleaved with the fourth and fifth
11          portions, the inner portion of the first of the
12          transverse coils interleaved with the first
13          portion, and the inner portion of the other of the
14          transverse coils interleaved with the fifth
15          portion.

1    56.    An inclined-turn axial coil assembly having an
2           axis defining and connecting a top and a bottom of

3       a central coil of the assembly, a first plane
4       containing the axis defining and separating a
5       front and a back of the assembly, the turns of the
6       central coil disposed so as to have substantially
7       reflectional symmetry with respect to a second
8       plane perpendicular to the axis and bisecting the
9       assembly, each of the turns being substantially
10      reflectionally symmetrical with respect to a third
11      plane perpendicular to the first and second
12      planes, the turns each defining a plane having an
13      angle of inclination defined by the intersection
14      with the second plane, the intersections of the
15      central coil turns all being to the front of the
16      assembly, and the angle of inclination increasing
17      for turns further and further from the second
18      plane, said turns extending to a first distance
19      from the second plane.

1    57.   The axial coil assembly of claim 56 further
2          comprising a pair of end coils at respective ends
3          of the central coil and more distant from the
4          second plane than said first distance, the turns
5          thereof each defining a plane with an angle of
6          inclination defined by the intersection with the
7          second plane, the intersections of the end coil
8          turns all being to the back of the assembly.

1    58.   The assembly of claim 56 in which said central
2          coil is substantially round in cross section.

1    59.   The assembly of claim 56 in which said central
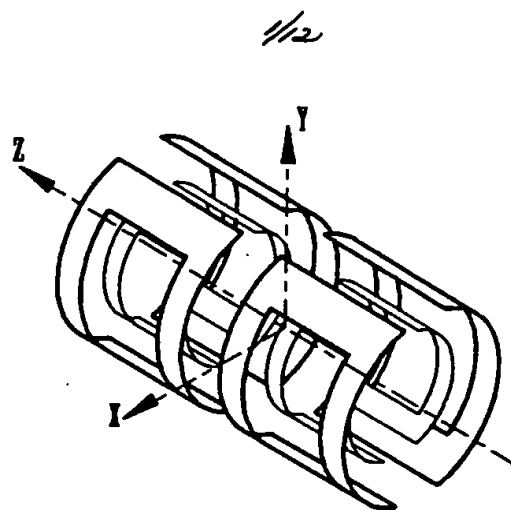2          coil is substantially trapezoidal in cross
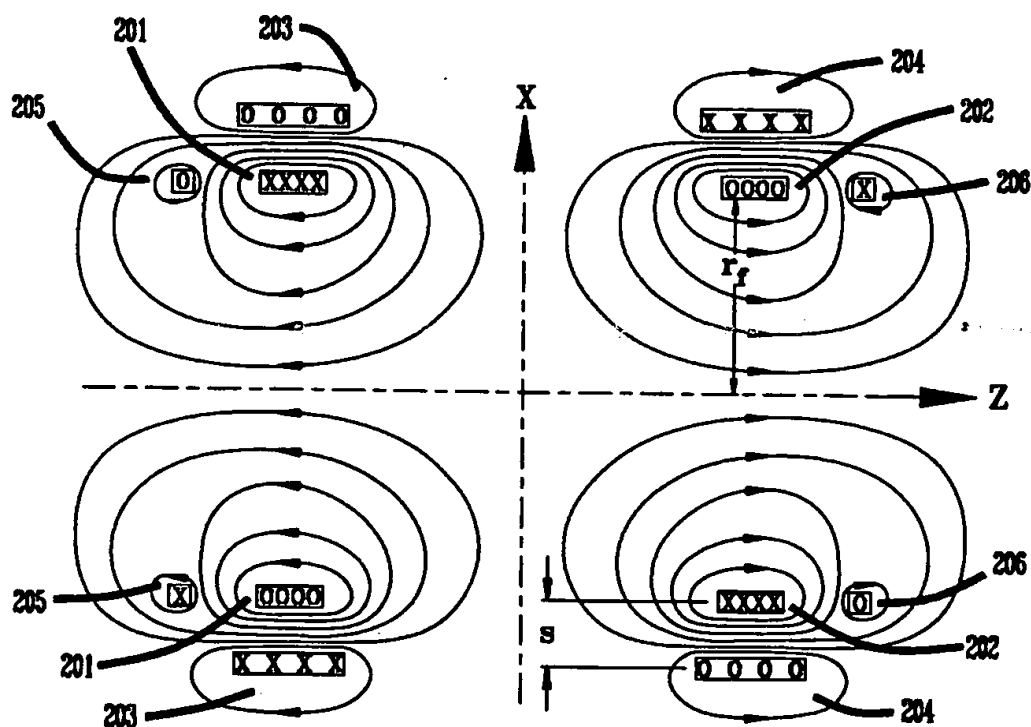3          section.

1    60.   The assembly of claim 56 further comprising a
2          coilform, said coilform made from a material

3          selected from the set consisting of alumina,
4          silicon nitride, zirconia, alumina-silica-boria
5          glasses, borosilicate glasses, machinable glasses,
6          plastic composites having at least 10% carbon
7          fiber content, plastic composites having more than
8          25% ceramic fiber content, and plastic composites
9          having density greater than 2.0 g/cm$^3$.

1    61.   A non-ferromagnetic transverse gradient coil
2          system having a central axis, said system
3          comprising:
4               an even number of solenoidal-like central
5          axial assemblies having a major diameter wound on
6          rigid coilforms having axial coil axes parallel to
7          said central axis and positioned such that the
8          distance between said central axis and each said
9          axial coil axis is greater than the major diameter
10         of said axial coils, the assemblies arranged
11         substantially symmetrical with respect to 180°
12         rotation about the central axis, the assemblies
13         being substantially symmetrical with respect to
14         reflection through a first plane perpendicular to
15         said central axis;
16              each of said assemblies further characterized
17         in that for each of said assemblies, its axial
18         coil axis defines and connects a top and a bottom
19         of a central coil of the assembly, a second plane
20         contains the axis defining and separating a front
21         toward the central axis and a back of the assembly
22         outward from the central axis, each of the turns
23         of the central coil of the assembly being
24         substantially reflectionally symmetrical with
25         respect to a third plane perpendicular to the
26         first and second planes, the turns each defining a
27         plane having an angle of inclination defined by
28         the intersection with the second plane, the

29      intersections of the central coil turns all being
30      toward the central axis, and the angle of
31      inclination increasing for turns further and
32      further from the second plane, said turns
33      extending to a first distance from the second
34      plane.

1   62. The system of claim 61 in which each of the said
2       assemblies further comprises a pair of end coils
3       at respective ends of the central coil and more
4       distant from the second plane than said first
5       distance, the turns thereof each defining a plane
6       with an angle of inclination defined by the
7       intersection with the second plane, the
8       intersections of the end coil turns all being
9       outward from the central axis.

1   63. The system of claim 61 in which each said central
2       coil is substantially round in cross section.

1   64. The system of claim 61 in which each said central
2       coil is substantially trapezoidal in cross
3       section.

1/12



Figure 1   Prior Art



Figure 2   Prior Art

Figure 3

3/2



Figure 4

4/12



Figure 5

5/12

Figure 6b

601

y

602

603

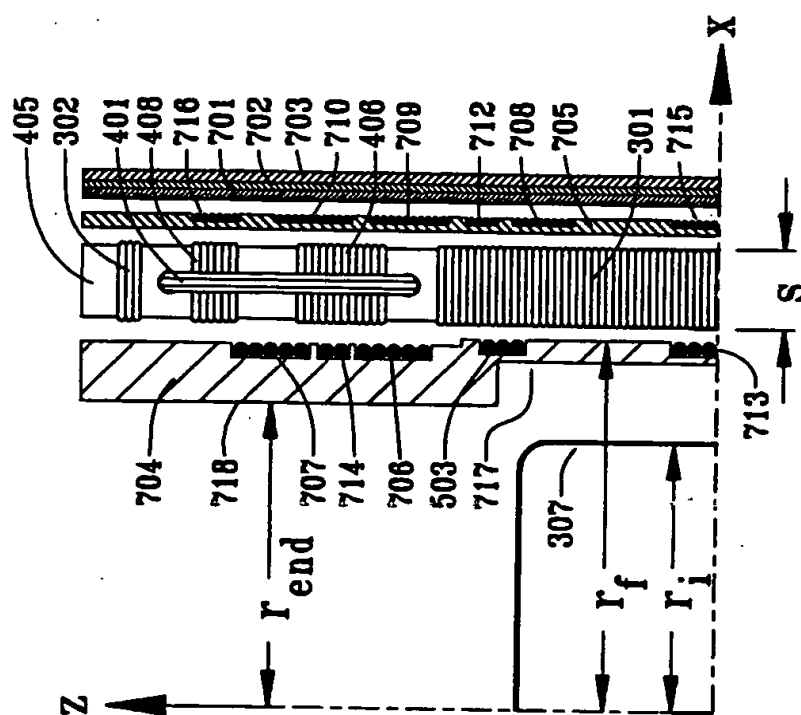x

Figure 6a

601

602

603

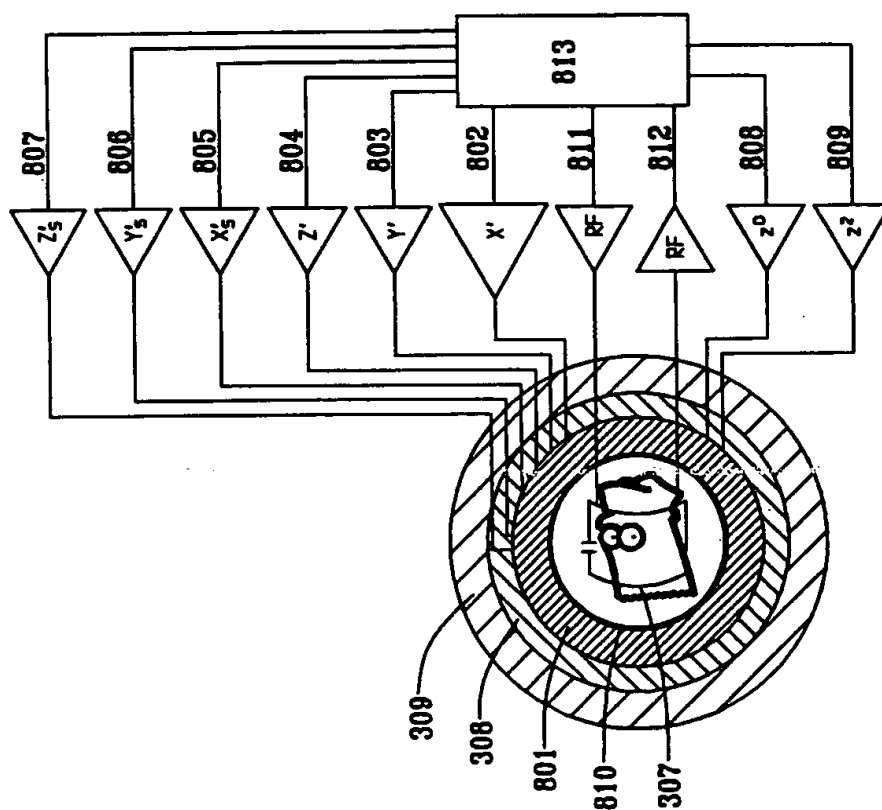601

602

603

z
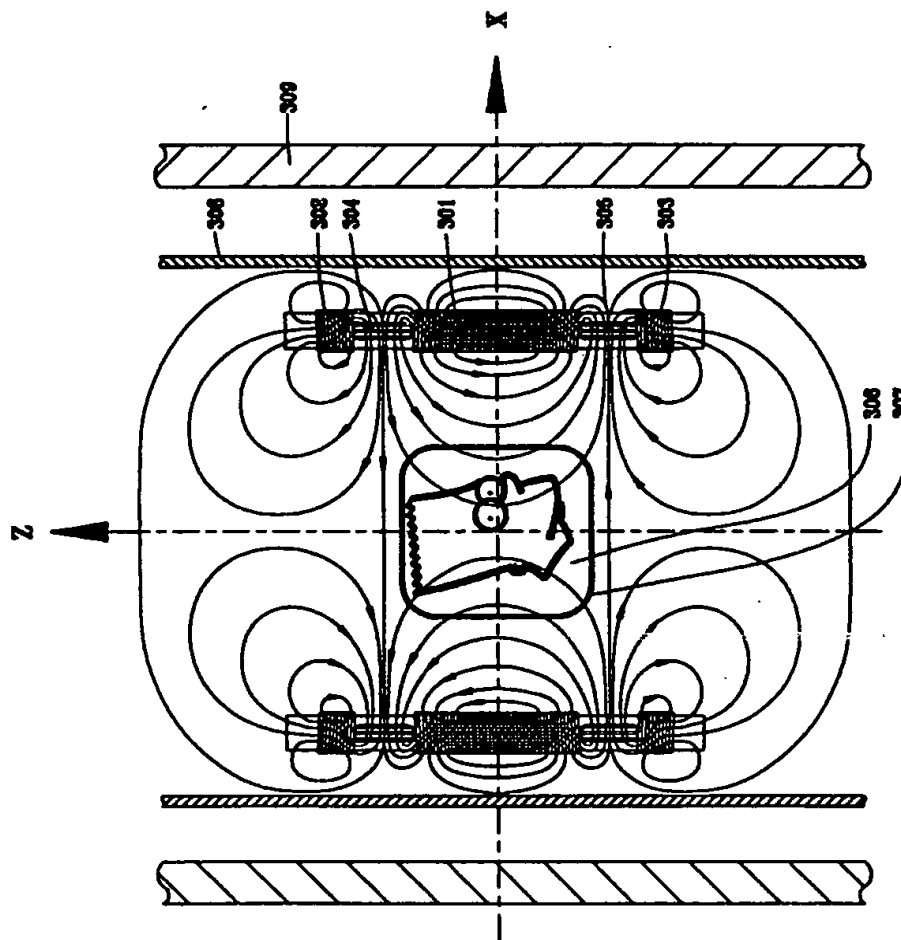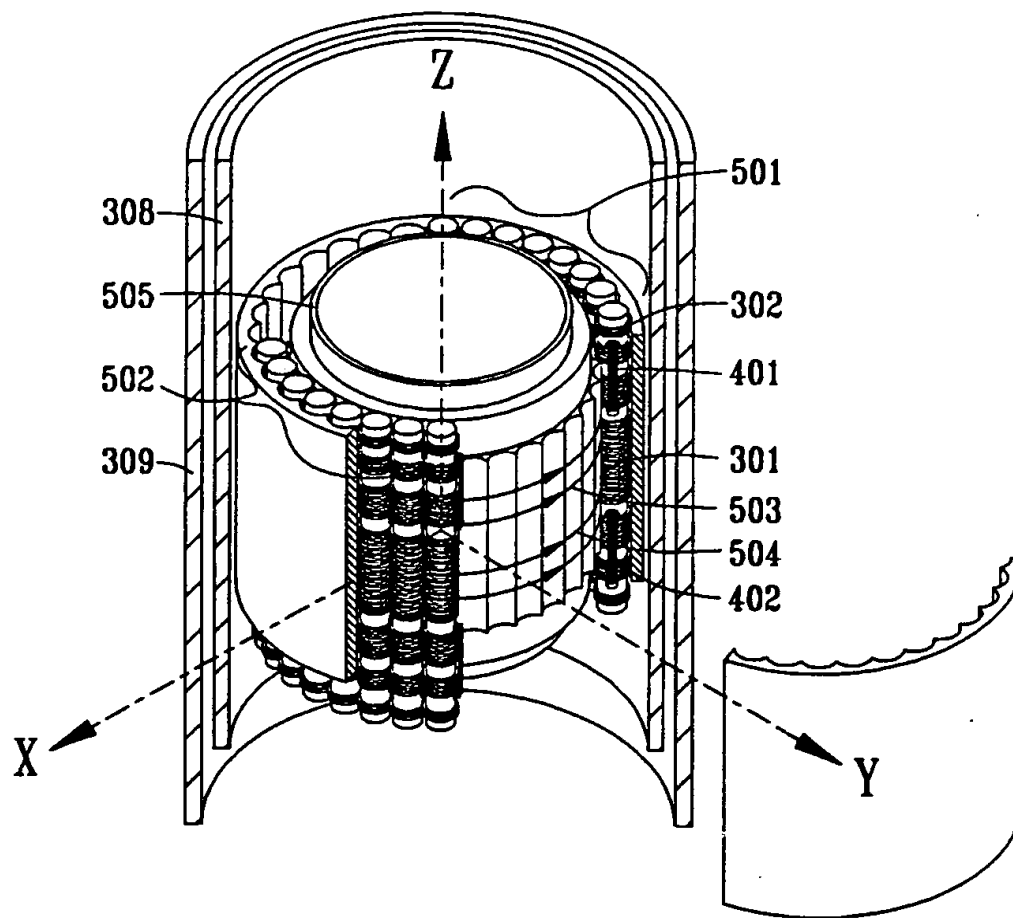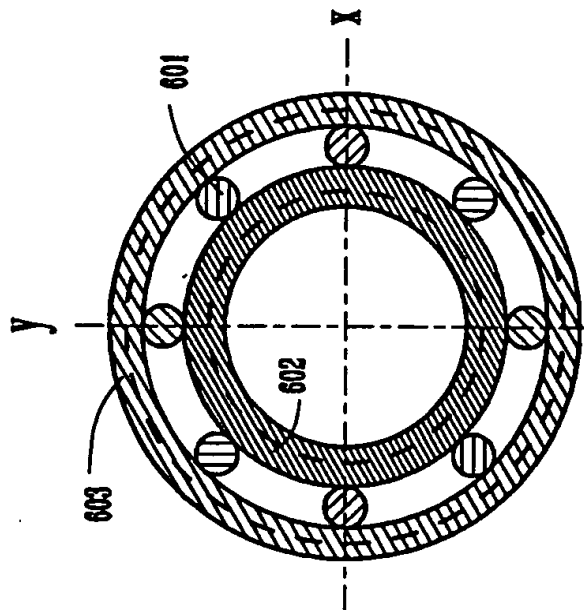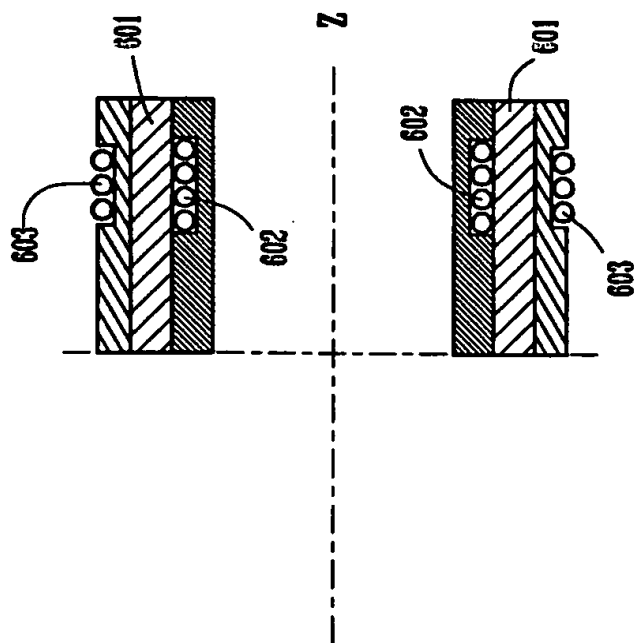
6/12



Figure 7
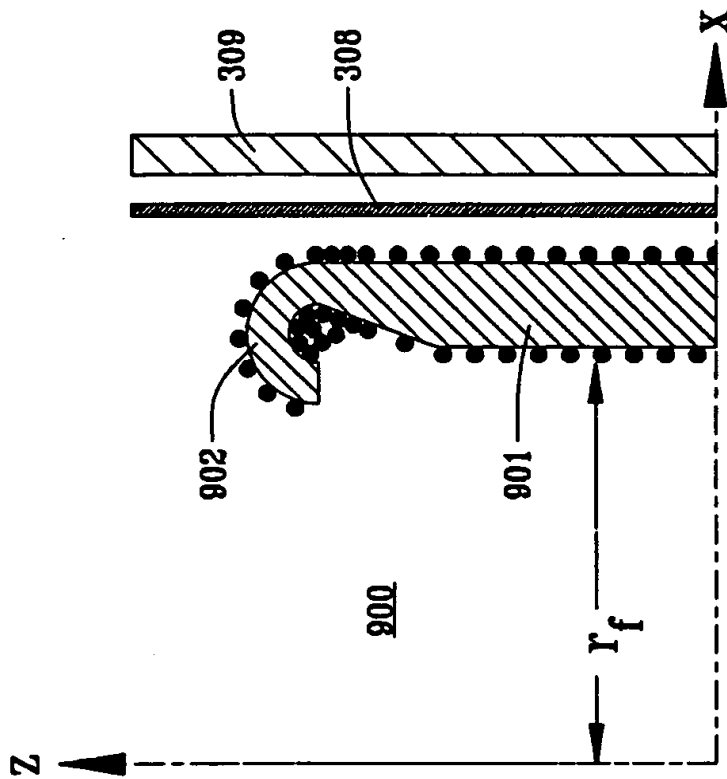
7/12



Figure 8

8/12



Figure 9

9/12
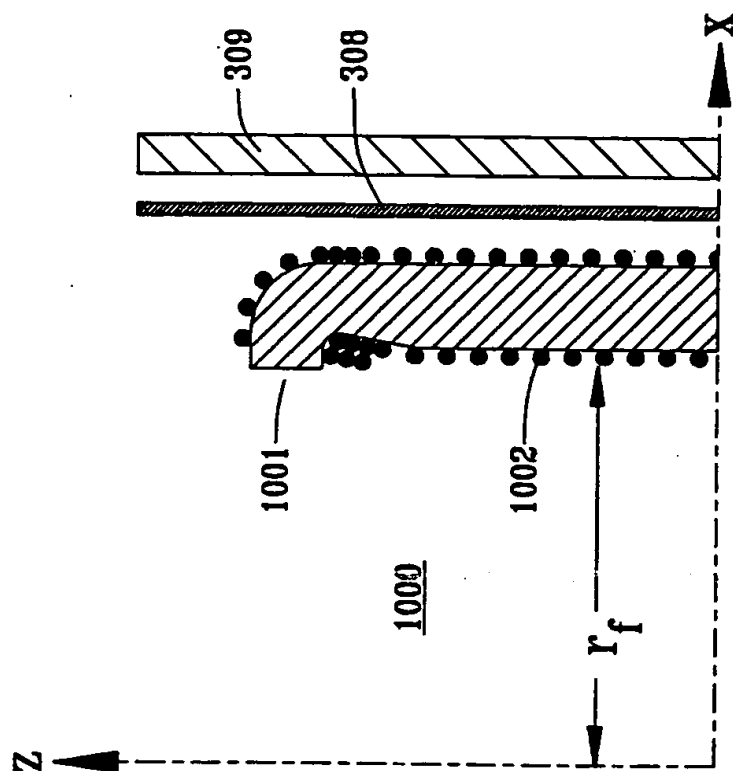


Figure 10

10/12
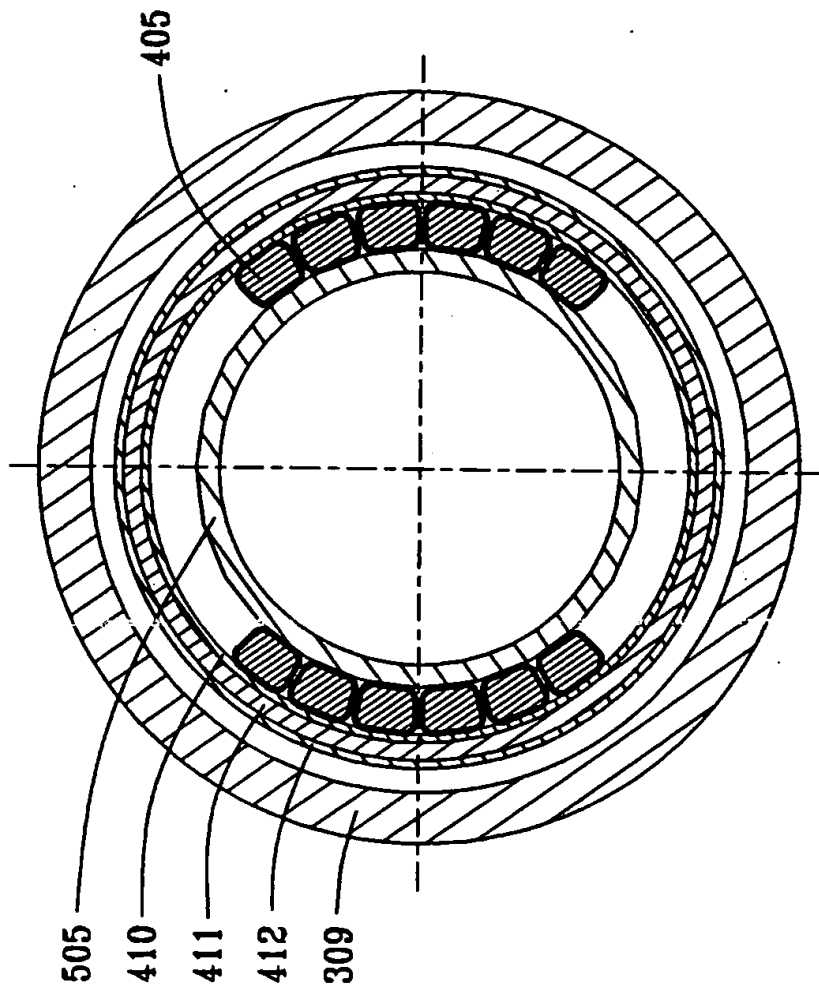

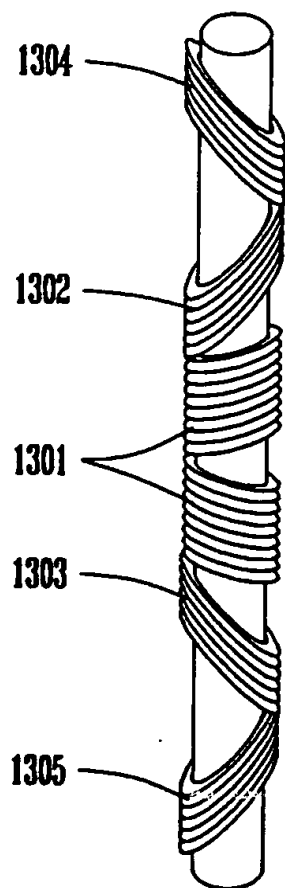
Figure 11

11/12
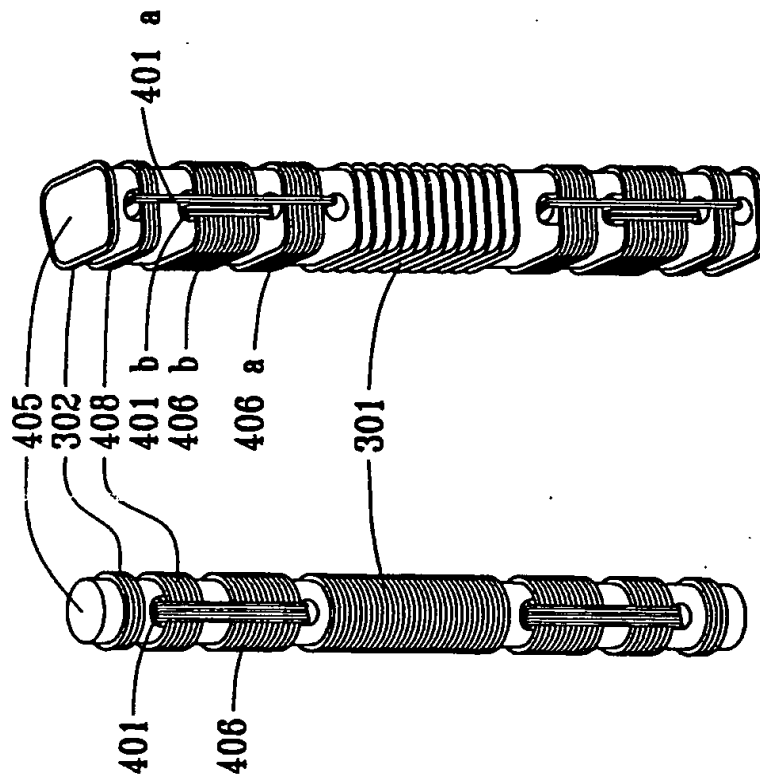


Figure 12a          Figure 12b

12/12

1304

1302

1301

1303

1305

# Figure 13

## INTERNATIONAL SEARCH REPORT

| | |
|---|---|
| **A. CLASSIFICATION OF SUBJECT MATTER** | |

IPC(5) :G01R 33/20
US CL :324/318, 322 300; 335/299; 336/225
According to International Patent Classification (IPC) or to both national classification and IPC

**B. FIELDS SEARCHED**

Minimum documentation searched (classification system followed by classification symbols)

U.S. : 324/318-322, 300; 335/282, 296-301; 336/180, 189, 199, 208, 225, 228

Documentation searched other than minimum documentation to the extent that such documents are included in the fields searched

Electronic data base consulted during the international search (name of data base and, where practicable, search terms used)

APS (Terms: shield, gradient, solenoid, rf)

**C. DOCUMENTS CONSIDERED TO BE RELEVANT**

| Category* | Citation of document, with indication, where appropriate, of the relevant passages | Relevant to claim No. |
|---|---|---|
| A | US, A, 4,910,462 (Roemer et al) 20 March 1990, See Fig. 1a. | 1-19 |
| A | US, A, 4,820,988 (Crooks et al) 11 April 1989, fig. 2. | 1-19 |
| A,P | US, A, 5,166,619 (Ries) 24 November 1992, figs. 3-4. | 1-19 |
| Y<br>A | US, A, 3,237,090 (Royer et al) 22 Febuary 1966, fig. 7. | 20-25,48<br>26-30 |

| | |
|---|---|
| [X] Further documents are listed in the continuation of Box C. | [ ] See patent family annex. |

| | |
|---|---|
| * Special categories of cited documents: | "T" later document published after the international filing date or priority date and not in conflict with the application but cited to understand the principle or theory underlying the invention |
| "A" document defining the general state of the art which is not considered to be part of particular relevance | |
| "E" earlier document published on or after the international filing date | "X" document of particular relevance; the claimed invention cannot be considered novel or cannot be considered to involve an inventive step when the document is taken alone |
| "L" document which may throw doubts on priority claim(s) or which is cited to establish the publication date of another citation or other special reason (as specified) | "Y" document of particular relevance; the claimed invention cannot be considered to involve an inventive step when the document is combined with one or more other such documents, such combination being obvious to a person skilled in the art |
| "O" document referring to an oral disclosure, use, exhibition or other means | |
| "P" document published prior to the international filing date but later than the priority date claimed | "&" document member of the same patent family |

| | |
|---|---|
| Date of the actual completion of the international search<br><br>21 October 1993 | Date of mailing of the international search report<br><br>26 NOV 1993 |
| Name and mailing address of the ISA/US<br>Commissioner of Patents and Trademarks<br>Box PCT<br>Washington, D.C. 20231 | Authorized officer<br><br>KENNETH WIEDER |
| Facsimile No. NOT APPLICABLE | Telephone No. (703) 305-4900 |

Form PCT/ISA/210 (second sheet)(July 1992)

| C (Continuation). DOCUMENTS CONSIDERED TO BE RELEVANT | | |
|---|---|---|
| Category* | Citation of document, with indication, where appropriate, of the relevant passages | Relevant to claim No. |
| Y<br>A | US, A, 2,498,475 (Adams) 21 February 1950, fig. 1. | 20-25, 48<br>26-30 |
| A | US, A, 3,924,211 (Ioffe et al) 02 December 1975, figs. 5-6 and 7-9. | 20-40 |
| A | US, A, 2,354,331 (Polydoroff) 25 July 1944, figs. 2 and 4. | 31-40 |
| Y | US, A, 4,514,586 (Waggoner) 30 April 1985, col. 2 lines 37-46. | 41 |
| Y | US, A, 4,920,011 (Ogawa et al) 24 April 1990, figs. 4-5. | 41 |
| Y,P | US, A, 5,132,621 (Kang et al) 21 July 1992, col. 10 line 35 to col. 11 line 35. | 41 |
| Y | US, A, 4,646,046 (Vavrek et al) 24 Febuary 1987, fig. 6. | 41 |
| Y | JP, A, 54-38792 (Hitachi) 23 March 1979, abstract. | 41 |
| Y | US, A, 4,768,008 (Purcell et al) 30 August 1988, figs. 3-4. | 43 |
| A | US, A, 4,935,714 (Vermilyea) 19 June 1990, fig. 4. | 43 |
| Y | US, A, 4,965,521 (Egloff) 23 October 1990, fig. 1a. | 44-45 |
| Y | US, A, 4,642,569 (Hayes et al) 10 February 1987, fig. 1. | 44-45 |
| A | US, A, 4,876,510 (Siebold et al) 24 October 1989, col 3 lines 24-25. | 43-45 |
| X | US, A, 4,733,189 (Punchard et al) 22 March 1988, fig. 4. | 46 |
| X<br>Y | US, A, 5,084,676 (Saho et al) 28 January 1992, fig. 1. | 46<br>47 |
| A,T | US, A, 5,235,283 (Lehne et al) 10 August 1993, fig 4. | 47 |
| Y | US, A, 4,954,781 (Hirata) 04 September 1990, fig. 18. | 47 |
| Y | US, A, 5,061,891 (Totsuka et al) 29 October 1991, figs. 6 and 8. | 48 |
| Y,P | US, A, 5,198,769 (Frese et al) 30 March 1993, fig. 5 | 56-64 |
| Y | US, A, 4,766,383 (F x et al) 23 August 1988, fig. 4b. | 56-64 |
| Y,P | US, A, 5,185,577 (Minemura) 09 February 1993, fig 9a. | 56-64 |
| A,T | US, A, 5,225,782 (Laskaris et al) 06 July 1993, fig. 1 | 46 |

**Box I    Observations where certain claims were found unsearchable (Continuation of item 1 of first sheet)**

This international report has not been established in respect of certain claims under Article 17(2)(a) for the following reasons:

1. ☐ Claims Nos.:
   because they relate to subject matter not required to be searched by this Authority, namely:

2. ☐ Claims Nos.: 42
   because they relate to parts of the international application that do not comply with the prescribed requirements to such an extent that no meaningful international search can be carried out, specifically:

   Please See Extra Sheet.

3. ☐ Claims Nos.:
   because they are dependent claims and are not drafted in accordance with the second and third sentences of Rule 6.4(a).

**Box II    Observations where unity of invention is lacking (Continuation of item 2 of first sheet)**

This International Searching Authority found multiple inventions in this international application, as follows:
         (Form PCT/ISA/206 Previously Mailed.)
   I.      Figs. 3-5, 7, 11 describe solenoids drawn to claims 1-19, 44-47.
   II.     Fig. 6 describes shields drawn to claims 41-43.
   III.    Fig. 9 describes c-coils drawn to claims 31-40.
   IV.     Fig. 10 describes u-coils drawn to claims 20-30.
   V.      Fig. 12 describes alternate solenoids drawn to claims 48-55.
   VI.     Fig. 13 drawn to inclined solenoids drawn to claims 56-64.

1. ☒ As all required additional search fees were timely paid by the applicant, this international search report covers all searchable claims.

2. ☐ As all searchable claims could be searched without effort justifying an additional fee, this Authority did not invite payment of any additional fee.

3. ☐ As only some of the required additional search fees were timely paid by the applicant, this international search report covers only those claims for which fees were paid, specifically claims Nos.:

4. ☐ No required additional search fees were timely paid by the applicant. Consequently, this international search report is restricted to the invention first mentioned in the claims; it is covered by claims Nos.:

**Remark on Protest**    ☐    The additional search fees were accompanied by the applicant's protest.
                         ☒    No protest accompanied the payment of additional search fees.

BOX L OBSERVATIONS WHERE CLAIMS WERE FOUND UNSEARCHABLE:

2. Where no meaningful search could be carried out, specifically:

Claim 42 lacks clarity under PCT article 6 because it is not clear whether "said element" (which lacks antecedent basis) are disposed at different radii at the same time, or if the element is used at $r_{min}$ and later at $r_{max}$. If said element is used in the former case, then it is unclear how the foil can have a radius between $r_{min}$ and $r_{max}$. Does the foil physically intersect said element? Moreover, there is no support for such an arrangement between said element and the foil.